Chinese Herbal Medicines 17 (2025) 108–126

Contents lists available at ScienceDirect

Chinese Herbal Medicines

journal homepage: www.elsevier.com/locate/chmed

Original Article

Cerbera odollam fruit extracts enhance anti-cancer activity of sorafenib in HCT116 and HepG2 cells

Supawadee Parhira [a,b,c], Orakot Simanurak [d], Khemmachat Pansooksan [b,e], Julintorn Somran [f], Apirath Wangteeraprasert [g], Zhihong Jiang [h], Liping Bai [h], Pranee Nangngam [i], Dumrongsak Pekthong [b,c,j,*], Piyarat Srisawang [b,d,k,*]

[a] *Department of Pharmaceutical Technology, Faculty of Pharmaceutical Sciences, Naresuan University, Phitsanulok 65000, Thailand*
[b] *Center of Excellence for Innovation in Chemistry, Naresuan University, Phitsanulok 65000, Thailand*
[c] *Center of Excellence for Environmental Health and Toxicology, Faculty of Pharmaceutical Sciences, Naresuan University, Phitsanulok 65000, Thailand*
[d] *Department of Physiology, Faculty of Medical Science, Naresuan University, Phitsanulok 65000, Thailand*
[e] *Department of Pharmaceutical Chemistry and Pharmacognosy, Faculty of Pharmaceutical Sciences, Naresuan University, Phitsanulok 65000, Thailand*
[f] *Department of Pathology, Faculty of Medicine, Naresuan University, Phitsanulok 65000, Thailand*
[g] *Department of Medicine, Faculty of Medicine, Naresuan University, Phitsanulok 65000, Thailand*
[h] *State Key Laboratory of Quality Research in Chinese Medicine, Guangdong-Hong Kong-Macao Joint Laboratory of Respiratory Infectious Disease, Macau Institute for Applied Research in Medicine and Health, Macau University of Science and Technology, Macau 999078, China*
[i] *Department of Biology, Faculty of Science, Naresuan University, Phitsanulok 65000, Thailand*
[j] *Department of Pharmacy Practice, Faculty of Pharmaceutical Sciences, Naresuan University, Phitsanulok 65000, Thailand*
[k] *Center of Excellence in Medical Biotechnology, Faculty of Medical Science, Naresuan University, Phitsanulok 65000, Thailand*

ARTICLE INFO

Article history:
Received 11 June 2024
Revised 22 August 2024
Accepted 19 November 2024
Available online 20 November 2024

Keywords:
apoptosis
Cerbera odollam Gaertn.
HCT116
HepG2
reactive oxygen species
sorafenib

ABSTRACT

Objective: While higher therapeutic doses of toxic cardiac glycosides derived from *Cerbera odollam* are frequently employed in cases of suicide or homicide, ongoing research is investigating the potential anticancer properties of low-concentration extracts obtained from the fruits of *C. odollam*. The present study aimed to determine the enhanced anticancer effects and minimize potential side effects of combining extracts from *C. odollam* fruits from Thailand with sorafenib against HCT116 and HepG2 cells.
Methods: The dried powder of fresh green fruits of *C. odollam* was fractionated, and its phytochemical contents, including total cardiac glycosides, phenolics, flavonoids, and triterpenoids, were quantified. The cytotoxic effects of these fractions were evaluated against HCT116 and HepG2 cells using the MTT assay. The fractions showing the most significant response in HCT116 and HepG2 cells were subsequently combined with sorafenib to examine their synergistic effects. Apoptosis induction, cell cycle progression, and mitochondrial membrane potential (MMP) were then assessed. The underlying mechanism of the apoptotic effect was further investigated by analyzing reactive oxygen species (ROS) generation and the expression levels of antioxidant proteins.
Results: Phytochemical analysis showed that *C. odollam*-ethyl acetate fraction (COEtOAc) was rich in cardiac glycosides, phenolics, and flavonoids, while the dichloromethane fraction (CODCM) contained high levels of triterpenoids and saponins. Following 24 h treatment, HCT116 showed the most significant response to COEtOAc, while HepG2 responded well to CODCM with IC_{50} values of (42.04 ± 16.94) μg/mL and (123.75 ± 14.21) μg/mL, respectively. Consequently, COEtOAc (20 μg/mL) or CODCM (30 μg/mL), both administered at sub-IC_{50} concentrations, were combined with sorafenib at 6 μmol/L for HCT116 cells and 2 μmol/L for HepG2 cells, incubated for 24 h. This combination resulted in a significant suppression in cell viability by approximately 50%. The combination of treatments markedly enhanced apoptosis, diminished MMP, and triggered G_0/G_1 phase cell cycle arrest compared to the effects of each treatment administered individually. Concurrently, increased formation of ROS and decreased expression of the antioxidant enzymes superoxide dismutase 2 and catalase supported the proposed mechanism of apoptosis induction by the combination treatment. Importantly, the anticancer effect demonstrated a specific targeted action with a favorable safety profile, as evidenced by HFF-1 cells displaying IC_{50} values 2–3 times higher than those of the cancer cells.
Conclusion: Utilizing sub-IC_{50} concentrations of COEtOAc or CODCM in combination with sorafenib can enhance targeted anticancer effects beyond those achieved with single-agent treatments, while mitigating

* Corresponding authors.
E-mail addresses: dumrongsakp@nu.ac.th (D. Pekthong), piyarats@nu.ac.th (P. Srisawang).

https://doi.org/10.1016/j.chmed.2024.11.007

opposing side effects. Future research will focus on extracting and characterizing active constituents, especially cardiac glycosides, to enhance the therapeutic potential of anticancer compounds derived from toxic plants.

1. Introduction

Cerbera odollam Gaertn., commonly referred to as one of the two Bintaro species alongside *C. manghas* L., is a tropical mangrove plant known for its toxicity. It is a member of the Apocynaceae family and is extensively found across Southeast Asia and commonly known as a pong-pong tree (Gaillard, Krishnamoorthy, & Bevalot, 2004). *C. manghas* is commonly found across various regions, including the islands of the Indian Ocean, tropical Asia, the Pacific Ocean islands, and tropical Africa (Maharana, 2021). *C. odollam* features elongated, dark green leaves that are lanceolate in shape. Its fruit is spherical and undergoes a color transformation from green to red as it ripens. Each fruit contains a seed, which is an ovoid kernel measuring approximately 2 cm × 1.5 cm (Fig. 1A–E) (Menezes et al., 2018).

C. odollam primarily contains deadly poisonous active cardenolides such as cerberin, cerbetin, cerberoside, cerdollaside, digitoxigenin, neriifolin, solanoside, tanghinigenin, tanghinin, and thevetin have been reported in *C. manghas* and *C. odollam*. Species of Apocynaceae with antiproliferative properties against human cancer cell lines include members of the genus *Cerbera*, with these compounds present in all parts (leaf, seed, and root) (Chan, Wong, & Chan, 2016). Additionally, the leaves of *C. odollam* have been found to contain cardiac glycosides, including 17 α-cerdollaside, 17 β-cerdollaside, cerleaside-α, and cerleaside-β, as well as tanghinigenin derivatives. The leaves and stems also yield lignans, such as olivil dimers, and iridoid triterpenes (Yunos, Osman, Jauri, Sallehudin, & Mutalip, 2020). The kernels contain the highest concentration of cerberin and are commonly used as agents for suicidal or homicidal, which has led to its colloquial names "suicide tree" or "pong-pong tree", despite its numerous medicinal benefits (Saxena et al., 2023). Leaves and bark of *C. odollam* possess cathartic properties, while latex is used as an emetic, purgative, and for irritant relief (Gaillard, Krishnamoorthy, & Bevalot, 2004). The fruit kernels are rich in toxins, including cerberin and other glycosides such as 17 α-neriifolin, and 17 β-neriifolin.

Cerberin inhibits the Na^+/K^+-ATPase in cardiac cells, causing elevated intracellular calcium due to the reduced activity of the passive sodium-calcium exchanger. This leads to a lengthening of the cardiac action potential, ultimately resulting in a decrease in heart rate and increase in inotropy (Yunos, Osman, Jauri, Sallehudin, & Mutalip, 2020). A variety of studies have indicated that individuals who commit suicide by consuming seeds from the pong-pong tree exhibit severe cardiac glycoside toxicity. This condition is marked by clinical manifestations including an irregular heartbeat accompanied by sinus bradycardia, hypotension, atrial flutter with variable atrioventricular block, and hyperkalemia levels surpassing 8 mEq/L (Fok, Victor, Bradberry, & Eddleston, 2018; Kassop et al., 2014; Menon, Kumar, & Jayachandran, 2016; Misek, Allen, LeComte, & Mazur, 2018; Nordt et al., 2020; Renymol, Palappallil, & Ambili, 2018; Rotella, Wong, Wong, & Graudins, 2020; Saxena et al., 2023; Wermuth, Vohra, Bowman, Furbee, & Rusyniak, 2018).

The research findings on the cytotoxic effects and potential therapeutic applications of extracts from *C. odollam* against various cancer cells have been extensively reported scientifically. Cardenolide glycosides, components of seed extracts from *C. odollam* exhibit potential anticancer against human breast cancer cells, human small-cell lung cancer, and human oral epidermoid carcinoma (Chantrapromma et al., 2003). Further investigation revealed *C. odollam* extracts had varying cytotoxic activities across different cancers (Gorantla, Vellekkatt, Nath, Anto, & Lankalapalli, 2014). Notably, cerberin demonstrated IC_{50} values more than a 20-fold specific cytotoxic effect in cancer cells compared to normal cells, suggesting its potential as a targeted anticancer agent (Hossan et al., 2019). Moreover, a novel cardenolide glycoside isolated from seeds of *C. odollam* exhibited cytotoxic effects on various cancer cells, including oral human epidermoid carcinoma KB, human breast cancer BC, and human small cell lung cancer NCI-H187 cells (Laphookhieo et al., 2004). Consequently, the results indicate that extracts from *C. odollam* could be among the most promising options for targeted anticancer treatments, providing substantial benefits for future cancer therapies (Menezes et al., 2018). The fruit kernels of *C. odollam* seeds contain several cardiac glycosides, including cerberin, cerberoside, and neriifolin, which can cause fatal cardiac glycoside toxicity. Elevated potassium levels correlate with increased mortality, particularly when serum digoxin levels exceed 1.3 ng/mL. Analysis of hepatic tissue and gastric fluid has demonstrated the presence of the cardiac glycosides cerberin and neriifolin following ingestion of pong-pong tree seeds in suicide attempts (Wermuth, Vohra, Bowman, Furbee, & Rusyniak, 2018).

Digoxin adverse effects including risk of mortality rate of about 19% have been observed when plasma digoxin concentration falls below 0.5 ng/L. Users with a maximum serum digoxin concentration exceeding 1.1 ng/mL exhibited an increased risk of all-cause mortality (Muk et al., 2020). Notably, a common reference range for serum digoxin is less than 1.2 ng/mL (Erkkilä, Hernesniemi, & Tynkkynen, 2023). The LD_{50} of digoxin was reported to be 5.5 mg/Kg in mice (Farghaly, Ashry, & Hareedy, 2018). Certain cardiac glycosides, including anvirzel, UNBS1450, PBI05204, and digoxin, have been recognized in clinical trials as potential cancer therapeutic agents. Furthermore, cardiac glycosides derived from plant extracts have demonstrated the ability to enhance the efficacy of anticancer medications against cancer cells, while displaying reduced cytotoxicity towards normal cells (Hou, Shang, Meng, & Lou, 2021).

Similar to digoxin, the utilization of *C. odollam* extracts in human subjects may encounter limitation due to a narrow therapeutic index, potentially leading to heightened incidences of side effects. Therefore, combining the extracts with chemotherapeutic drugs would present a more appropriate approach to harness their anticancer properties in the future, while concurrently ensuring safety applicability (Yunos, Osman, Jauri, Sallehudin, & Mutalip, 2020). Sorafenib is the frontline standard chemotherapy for numerous cancers, demonstrating superior efficacy in cancer treatment compared to alternative chemotherapy regimens when administered as a monotherapy. Its combination with other agents exhibited enhanced survival rates in advanced hepatocellular carcinoma (Cheng et al., 2022; Qin et al., 2021). By synergistically engaging with other anticancer agents, sorafenib combinations have demonstrated potential anticancer activity compared to sorafenib monotherapy, which often are administered below the toxic threshold, thereby resulting in a reduction

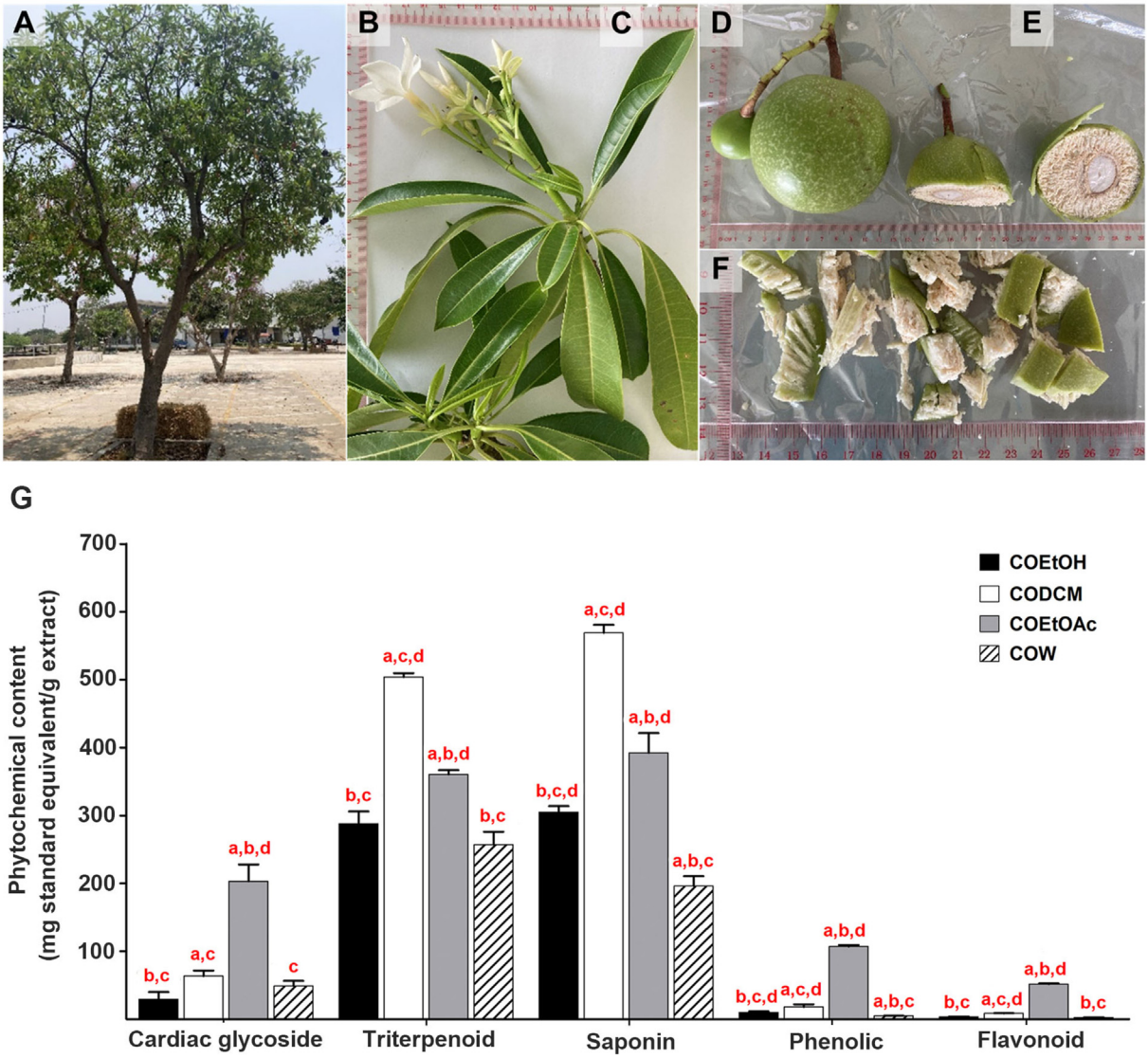

Fig. 1. Appearance of *C. odollam*. (A) Tree, (B) flower, (C) leaves, (D) green whole fruit, (E) cross section of fruit and (F) chopped fruit. (G) Phytochemical content of extracts from fruits of *C. odollam*: total cardiac glycoside (mg DXE/g extract), total triterpenoid content (mg UAE/g extract), total saponin content (mg OLE/g extract), total phenolic content (mg GAE/g extract), and total flavonoid content (mg RTE/g extract). COEtOH, CODCM, COEtOAc and COW were ethanolic crude extract, dichloromethane fraction, ethyl acetate fraction, and water fraction of fruits of *C. odollam*, respectively. The data, presented as mean ± SD from three independent experiments, were analyzed to investigate significant differences using One-way ANOVA and *t*-test, unequal variance with Bonferroni correction. $^{a}P < 0.05$ *vs* COEtOH group, $^{b}P < 0.05$ *vs* CODCM group, $^{c}P < 0.05$ *vs* COEtOAc group, and $^{d}P < 0.05$ *vs* COW group.

of sorafenib side effects (Li et al., 2021c; Taha, Aboulwafa, Zedan, & Helmy, 2022; Wang et al., 2022b). Therefore, a combination strategy of sorafenib with potential anticancer agents can overcome clinical limitations, augmenting clinical efficacy and safety of usage.

The objective of the present study was to explore the enhanced anticancer potential of fruit extracts from *C. odollam* in Thailand in combination with sorafenib, both administered at concentrations below their IC_{50} values, against HCT116 and HepG2 cells. The mechanism of action was explored, focusing on apoptosis induced by reactive oxygen species (ROS)-mediated oxidative damage because of the combination therapy. This finding provides essential knowledge for the development of novel anticancer treatments, highlighting the potential of using low concentrations of both toxic herbal extracts and chemotherapy drugs to enhance therapeutic efficacy while minimizing adverse side effects.

2. Materials and methods

2.1. Plant materials

The fresh green fruits of *C. odollam* (Fig. 1) were collected from a garden in Naresuan University (latitude 16.737 745, longtitude 100.198 738), Phitsanulok, Thailand, during June 2018–2022. The fresh green fruits without seed of *C. odollam* (22 kg) were chopped into small pieces (Fig. 1F), then dried in a hot air oven at (45 ± 5) °C for around 72 h and blended to yield its dried fruit powders. The dry powder of *C. odollam* fruit was stored in a tight plastic bag and kept in a tight plastic box at ambient temperature (30 ± 5) °C until extraction. The plant used in this study was authenticated by one of the authors, Dr. Pranee Nangngam, a taxomonist. The voucher specimen (003823) was deposited at a PNU herbarium, Department of Biology, Naresuan University, Phitsanulok, Thailand. The collection of plant parts and their utilization for research

objectives was approved in accordance with the Plant Varieties Protect Act B.E. 2542 (1999), section 53, under permission number 0279/2563 from the Department of Agriculture, Ministry of Agricultural and Cooperatives, Thailand.

2.2. Sample preparation

The dry powder of *C. odollam* green fruits (2.0 kg) was marinated in 95% ethanol (Food grade, Liquor liquor distillery organization, Chachoengsao, Thailand) and then extracted by using ultrasonic-assisted extraction (40 kHz, Shenzhen Jie Tai Ultrasonic Cleaning Equipment Co., Ltd., Shenzhen, China) at room temperature (27 ± 5) °C for 30 min. The mixture was filtered through clean cotton cloth before passing through Whatman No.1 filter paper to obtain an ethanol solution for further evaporation using a rotary evaporator (Buchi, Flawil, Switzerland) at 50 °C to gain ethanolic crude extract of *C. odollam* (COEtOH). The plant residue was repeated extraction for two more times. COEtOH (200 g) was subjected to liquid–liquid partition between water (400 mL) and dichloromethane (600 mL). The dichloromethane layer was then separated from the water layer. The remaining water layer was subsequently fractionated with ethyl acetate (600 mL). The ethyl acetate layer was separated from the water layer. Each solvent was fractionated three times. The combined dichloromethane and ethyl acetate layers from three times fractionation were evaporated under vacuum at 50 °C until dry, yielding the dichloromethane fraction (CODCM) and ethyl acetate fraction (COEtOAc). The remaining water layer was evaporated to remove solvent for one hour then frozen and dried by freeze-drying machine (Martin Christ, Gamma 2–16 LSC model, Osterode am Harz, Germany) to obtain water fraction of *C. odollam* (COW). All *C. odollam*'s samples were stored in amber glass bottles and kept in refrigerator (4 ± 2) °C until used. The yield percentages for each fraction were determined by comparing them to 100 g of dried plant material.

2.3. Phytochemicals quantitative analysis

Total cardiac glycoside, phenolic, flavonoid and triterpenoid contents were performed using colorimetric method described previously by Sawong et al. (2022). In summary, the quantification of cardiac glycosides in *C. odollam* samples was conducted utilizing Baljet's reagent, with results expressed as milligrams (mg) of digoxin (Sigma-Aldrich, St Louis MO, USA) equivalent (DXE)/gram (g) of extract. Additionally, the phenolic content was assessed using Folin-Ciocalteu's reagent (Merck KGaA, Darmstadt, Germany), reported in terms of mg of gallic acid equivalent (GAE)/g of extract. Total flavonoid content was investigated using aluminum chloride solution and reported as mg of rutin (Sigma-Aldrich, St Louis MO, USA) equivalent (RTE)/g of extract. Total triterpenoid content [mg ursolic acid (Tokyo Chemical Industry, Tokyo, Japan) equivalent (UAE)/g extract] was determined by using 5% vanillin-acetic acid in glacial acetic acid solution then interacted with sulfuric acid. Total saponin content was performed by the method described by Lim et al. (2020) and Medina-Meza et al. (2016). In summary, sample solution (1 mg/ mL in acetic acid, 0.25 mL) was combined with one mL of a reagent mixture composed of glacial acetic acid (LabScan, Bangkok, Thailand) and sulfuric acid in a 1:1 vol ratio. The mixture was rigorous mixed followed by heat at 60 °C in a water bath for 30 min and then cooled down at ambient temperature (27 ± 5) °C. The absorbance of the sample was measured at a wavelength of 527 nm using a UV–VIS spectrophotometer (Shimadza Europa Gmbh, Duisburg, Germany). Oleanolic acid (Tokyo Chemical Industry, Tokyo, Japan) was used as a standard (0–175 μg/mL). Total saponin content was expressed as mg oleanolic acid equivalent (OAE)/g extract.

2.4. High performance liquid chromatography (HPLC) fingerprint

Four samples of *C. odollam*'s fruit extracts were dissolved in methanol (5 mg/mL) then filtered by 0.45 μm Nylon syringe filter. Samples solutions were injected to a photodiode array detector (PDA)-HPLC (Shimadzu PDA, Kyoto, Japan) using conditions described by Yang et al. (2016) with some modifications. The ACE column® (C_{18}, 150 mm × 4.6 mm, 5 μm) was used as a stationary phase. The gradient mobile phase system was water (A) and acetonitrile (B) (0–5 min, 5%–26% B; 5–30 min, 26%–35% B; 30–35 min, 35%–56% B; 35–40 min, 56%–56% B; 40–45 min, 56%–5% B; 45–50 min, 5%–5% B). The flow rate and the injection volumes were 0.6 mL/min and 20 μL, respectively. The wavelength (at 287 nm) and column temperature (25 °C) were set. The HPLC fingerprint of each sample was established by major peaks appearing in HPLC chromatogram at each retention time along with their purity index analyzed by the HPLC software (1.00 means purity is high, the number near 0.00 means the purity is low).

2.5. Cell culture

Cell lines utilized in this study included colon cancer HCT116 cells (RCB2979) purchased from the RIKEN BioResource Research Center (BRC) Cell Bank (Ibaraki, Japan), human hepatocellular carcinoma HepG2 cells (JCRB1054) purchased from Japanese Collection of Research Bioresources (JCRB) Cell Bank (Osaka, Japan), and normal human fibroblast HFF-1 cells (SCRC-1041) purchased from American Type Culture Collection (ATCC) (Virginia, USA). These cell lines were cultured in a complete growth medium, Dulbecco's modified Eagle's medium (DMEM) (Gibco, Thermo Fisher Scientific, Massachusetts, USA), upplemented with 10% fetal bovine serum (FBS, Capricorn Scientific, Ebsdorfergrund, Germany). Cells were maintained under incubated conditions of 37 °C with 5% CO_2 in a humidified incubator.

2.6. Cell proliferation assay

The cell viability assay dye, 3-(4,5-dimethylthiazol-2-yl)-2,5-diphenyltetrazolium bromide (MTT, D0801, Tokyo Chemical Industry CO., Ltd., Tokyo, Japan) was used to assess viable cells for a 24 h of the treatment. Cells were inoculated on 96-well plate at 1×10^4 cells/well, after a 24-hour incubation, cells were treated with the extracts at varying concentrations for 24 h at 37 °C in a 5% CO_2 incubator. For the combination assay, four concentrations of COEtOAc and CODCM fractions were selected based on sub-IC_{50} values of each fraction, with both cell lines incubated for 24 and 48 h. Detailed information on experimental incubation times was provided in each of the following methods and results sections. After that, cells were incubated with MTT solution at 2 mg/mL under 37 °C. The yellow color of MTT indicates viable cells with active mitochondrial reductase enzyme, which produces a violet color upon conversion into formazan crystals. After dissolving the crystals with dimethyl sulfoxide (DMSO), the solution was measured for absorbance at 595 nm using a microplate reader (BioTek Synergy, Agilent, California, USA). The percentage of cell viability was calculated using GraphPad Prism 9 software (GraphPad Software, Massachusetts, USA).

2.7. Apoptosis assay by flow cytometry

Apoptosis was assessed by staining cells with the impermeable Annexin V/Alexa Fluor 488 conjugate (A13201, Invitrogen, Thermo Fisher Scientific, Massachusetts, USA), which binds to phosphatidylserine (PS) exposed on the outer membrane during the early apoptotic stage, and propidium iodide (PI) (P3566, Invitrogen, Thermo Fisher Scientific, Massachusetts, USA), which labels

double-stranded DNA exposed due to impaired cell membrane permeability in the late apoptotic stage. This assessment was conducted after a 24-hour treatment period. Apoptotic cells were quantified using CytoFLEX flow cytometry, analyzed with CytExpert software (Version 2.4.0.28) (Beckman Coulter, California, USA), and calculated in percentage values of apoptotic cells with GraphPad Prism9 software.

2.8. Cell cycle arrest assay by flow cytometry

Following a 24-hour exposure to the extracts, the cells were fixed using cold 70% ethanol and subsequently treated with RNase A (AMRESCO LLC, A VWR Company, Ohio, USA). This was followed by the application of PI to stain double-stranded DNA, facilitating the evaluation of the cell cycle. Detection was performed using CytoFLEX flow cytometry and analyzed with CytExpert software. Percentages of cells in different cell cycle stages were calculated using GraphPad Prism9 software.

2.9. Mitochondrial membrane potential (MMP) assessment using flow cytometric analysis and fluorescence visualization

After treating the cells for 24 h, MMP was measured as part of the apoptotic pathway using 5,5′,6,6′-tetrachloro-1,1′,3,3′-tetrae thylbenzimidazolylcarbocyanine iodide (JC-1) (T3168, Invitrogen, Thermo Fisher Scientific, Massachusetts, USA). The MMP status was quantitatively evaluated with CytoFLEX flow cytometry and CytExpert software, and alterations were calculated as percentages using GraphPad Prism9 software. Additionally, MMP alterations were detected by staining cells with 4′,6-diamidino-2-phenylin dole, dihydrochloride (DAPI) (Invitrogen, Thermo Fisher Scientific, Massachusetts, USA) and JC-1 dye after fixing the cells with 4% formaldehyde for 15 min at room temperature, followed by fluorescence visualization using fluorescence microscopy (BX53F2, Olympus Corporation, Tokyo, Japan).

2.10. Assessment of reactive oxygen species (ROS) by flow cytometric analysis and fluorescence visualization

After treating the cells for 24 h, intracellular ROS formation assessment was conducted using 2′,7′-dichlorodihydrofluorescein diacetate (H2DCFDA) (Invitrogen, Thermo Fisher Scientific, Massachusetts, USA). Upon conversion to the fluorescent 2′,7′-dichloro fluorescein (DCF) product, ROS levels were quantitively detected using CytoFLEX flow cytometry and CytExpert software and calculated using GraphPad Prism9 software. Additionally, intracellular ROS production was also detected by incubating cells with H2DCFDA and counterstaining with DAPI after fixing the cells with 4% formaldehyde for 15 min at room temperature. Fluorescence visualization was conducted using fluorescence microscopy.

2.11. Western blot analysis

After treating the cells for 24 h, intracellular proteins were extracted using Mammalian Protein Extraction Reagent (M−PER; Thermo Fisher Scientific, Massachusetts, USA) with the addition of proteinase inhibitor cocktail (HiMedia Laboratories Private Limited, Maharashtra, India). Protein concentration was quantified using bicinchoninic acid assay reagent (Thermo Fisher Scientific, Massachusetts, USA) and measuring the absorbance at 590 nm. Subsequently, equal amounts of protein were separated using sodium dodecyl sulfate–polyacrylamide gel electrophoresis. Proteins were then transferred onto polyvinylidene fluoride membrane and blocked for non-specific binding with blocking solution (GeneDireX, Inc., Taiwan, China). The membrane was then incubated overnight at 4 °C with primary antibodies, including rabbit polyclonal superoxide dismutase 2 (SOD2)/manganese superoxide dismutase (MnSOD) (AF5144, Affinity bioscience, Ohio, USA), rabbit polyclonal catalase (DF7545, Affinity bioscience, Ohio, USA), and mouse monoclonal β-actin (8H10D10, Cell Signaling Technology, Inc., Massachusetts, USA). Following the washing step, horseradish peroxidase (HRP)-conjugated goat anti-rabbit or anti-mouse secondary antibodies (Life Technologies, Invitrogen, Thermo Fisher Scientific, Massachusetts, USA) were introduced, and the protein expression was subsequently visualized using the Luminata Forte Western HRP substrate (Merck KGaA, Darmstadt, Germany). Protein bands were quantitatively detected using chemiluminescence western blot detection (Image Quant LAS 4000; GE Healthcare Bio-Sciences AB, Uppsala, Sweden), and the relative expression levels were compared to β-actin (%) using the Image J software (version 1.46) and GraphPad Prism9 software.

2.12. Statistically analysis

Data presented were calculated as the mean ± SD values. The differences between the experimental and control groups were evaluated for statistical significance at $P < 0.05$ through One-way analysis of variance (ANOVA) or Student's *t*-test. This was complemented by Bonferroni's post hoc analysis for quantitative data processed in Microsoft Excel 2019, while Tukey's post hoc analysis (HSD) was employed for the cell culture experiments utilizing GraphPad Prism9 software.

3. Results

3.1. Extraction, phytochemical content and HPLC fingerprint

The preparation of the dry powder from *C. odollam* involved the initial chopping of 22 kg of fresh green fruits, which were subsequently subjected to drying in a hot air oven at a temperature of (45 ± 5) °C for approximately 72 h. Following this drying process, the material was blended, resulting in the production of about 2 kg (9.1%) of dry powder derived from the fresh fruit. This dry powder was then subjected to extraction using 95% ethanol, which was followed by liquid–liquid fractionation. This procedure yielded various fractions: COEtOH (10.5%), CODCM (1.85%), COEtOAc (0.30%), and COW (6.3%) of the dry plant material.

These four fractions were quantified for their phytochemicals by colorimetric assays, as shown in Fig. 1G. The total cardiac glycoside content (mg DXE/g extract) of COEtOAc (203.29 ± 24.70) was significantly higher than those of CODCM (63.50 ± 8.12), COW (48.71 ± 7.86), and COEtOH (29.54 ± 10.63). Similar trends were observed in the total phenolic (mg GAE/g extract) and total flavonoid contents (mg RTE/g extract) of COEtOAc (107.07 ± 2.16 and 51.71 ± 1.01), which were significantly higher than those of CODCM (18.18 ± 3.78 and 8.65 ± 0.41), followed by COEtOH (9.93 ± 1.51 and 3.33 ± 0.53), with the lowest value observed in COW (5.06 ± 0.17 and 2.50 ± 0.39). The total triterpenoid (mg UAE/g extract) and total saponin contents (mg OAE/g extract) of CODCM (504.17 ± 5.54 and 568.86 ± 12.10) were the highest values, significantly higher than those in COEtOAc (360.51 ± 6.40 and 392.31 ± 29.07), COEtOH (287.98 ± 18.11 and 305.13 ± 8.88) and COW (257.20 ± 18.84 and 195.97 ± 14.63).

The HPLC fingerprints of four fractions from *C. odollam* were illustrated with different characteristics in Fig. S1. Three major peaks were found in COEtOH. Interestingly, the peaks at 10.584 and 21.384 min showed their purity indexes at 0.999 and 0.943, respectively. The CODCM showed the highest peaks number up to five peaks with high values of purity indexes (0.97–1.00) at the retention times of 10.090, 16.380, 21.617, 23.305, and 35.431 min, and one peak at 7.500 min with the purity index

0.684. It showed that one major peak of COEtOAc, with a purity index 0.99, appeared at the retention time of 20.965 min, while the peak at 7.400 min had low purity index value. However, the conditions used in this study did not adequately separate compounds in COEtOAc eluted around 10–15 min, resulting in a broad peak. Two major peaks at 2.800 and 4.110 min, each with purity index of 0.99, were found in an HPLC chromatogram of COW.

3.2. Examination of antiproliferative effect of C. odollam fruit extracts on HCT116 and HepG2 cells by MTT analysis

Data presented in Fig. 2, demonstrating the results of MTT assay after 24 h of treatment, indicated that HCT116 exhibited the highest significant response to COEtOAc, with an IC_{50} value of 38.48 ± 7.94 μg/mL, in contrast, HepG2 response favorably to CODCM, yielding an IC_{50} value of 123.75 ± 14.21 μg/mL, when compared to the other extract fractions. Consequently, COEtOAc and CODCM were selected to study their antiproliferative effects in combination with sorafenib in HCT116 and HepG2 cells. The study aimed to assess the effectiveness of these treatment combinations at low doses to minimize potential side effects while maintaining the anticancer efficacy. The IC_{50} values of sorafenib, following a 24-hour incubation period, were approximately 5–18 μmol/L for HCT116 cells and 13–20 μmol/L for HepG2 cells (Alsulaimany et al., 2023; Elwan et al., 2022; Hsu et al., 2016; Hu et al., 2022; Ismail et al., 2023; Taha et al., 2022; Talezadeh Shirazi et al., 2022; Walker et al., 2009; Yao et al., 2012; Zhang et al., 2019).

Four concentrations of COEtOAc and CODCM fractions, selected within or near the IC_{50} values of each fraction, were used in a combination experiment (Fig. 3A–D). COEtOAc at 5, 10, 20, and 40 μg/mL was tested on HCT116 cells, and CODCM at 5, 15, 30, and 60 μg/mL was tested on HepG2 cells following a 24-hour incubation period. The minimum concentrations of sorafenib showing significant differences from the vehicle control after 24 h were 3 μmol/L in HCT116 cells and 2 μmol/L in HepG2 cells. In HCT116 cells, the combination of COEtOAc at 20 μg/mL with 3 μmol/L of sorafenib, both at half-IC_{50} concentrations for a 24-hour treatment, resulted in a less pronounced response compared to doubling the sorafenib concentration to 6 μmol/L. The treatment with 6 μmol/L sorafenib alone led to a 20% cell death rate in HCT116 cells. Extending the incubation period to 48 h with 20 μg/mL of COEtOAc and 6 μmol/L of sorafenib exhibited a stronger response than the 24-hour incubation. The combination of COEtOAc at 20 μg/mL and 6 μmol/L of sorafenib for a 24-hour treatment in HCT116 cells, demonstrated a 50% inhibition of cell viability, thereby indicating these concentrations and incubation times were suitable for further study into the mechanism of cytotoxic effects.

The combination of CODCM at 30 μg/mL with 2 μmol/L of sorafenib, both below their respective half-IC_{50} values, significantly reduced cell viability after 24–48 h of incubation in HepG2 cells (Fig. 3E–F). HepG2 cells showed only a 10% inhibition of viability when treated with 2 μmol/L sorafenib alone. Doubling the concentration of sorafenib to 4 μmol/L while maintaining CODCM at 30 μg/mL for 24–48 h further enhanced the reduction in cell viability compared to the individual effects of CODCM or sorafenib treatments. Moreover, the combination of CODCM at 30 μg/mL with 2 μmol/L of sorafenib after 24 h of treatment resulted in a 50% inhibition of cell viability. These findings indicated that these specific concentrations and incubation times were suitable for further investigation into the cytotoxic mechanisms in HepG2 cells.

A quantitative analysis of synergy and combination index (CI) calculations, performed using CalcuSyn software (Wang et al., 2021), demonstrated the synergistic activity, indicated by a CI value of less than 1. Specifically, 6 μmol/L of sorafenib combined with 20 μg/mL of COEtOAc in HCT116 cells yielded a CI value of 0.850, while 2 μmol/L of sorafenib combined with 30 μg/mL of CODCM in HepG2 cells produced a CI value of 0.557, both within a 24-hour incubation period (Table S1).

These results demonstrate that sub-IC_{50} concentrations of both COEtOAc and CODCM, when combined with sub-IC_{50} concentrations of sorafenib, can enhance the targeted anticancer effects.

3.3. Analysis of apoptosis, MMP, cell cycle arrest, and formation of ROS following treatment with C. odollam fruit extracts combined with sorafenib on HCT116 and HepG2 cells

In the flow cytometric analysis, a combination of 20 μg/mL of COEtOAc with 6 μmol/L of sorafenib in HCT116 for a 24-hour incubation showed a significant increase in apoptosis and a decrease in MMP compared to the independent treatment of either COEtOAc or sorafenib (Fig. 4A–D). The combined treatment resulted in an arrest of the cell cycle at the G_2/M phase, similar to the effects seen with COEtOAc treatment alone, whereas sorafenib treatment did not induce any changes in the cell cycle phases (Fig. 4E–F). Additionally, following the combination treatment, there was a notable increase in ROS production when compared to the individual treatments (Fig. 4G–H).

Similar to the findings in HCT116 cells, a combination of 30 μg/mL of CODCM with 2 μmol/L of sorafenib in HepG2 cells significantly increased apoptosis with a decrease in MMP after a 24-hour incubation period (Fig. 5A–D). The integrated treatment approach demonstrated a G_2/M phase cell cycle arrest, akin to the effects observed with CODCM treatment alone, whereas the application of sorafenib did not result in any changes to the cell cycle phase (Fig. 5E–F). Additionally, ROS formation following the combination treatment significantly increased compared to the single treatment (Fig. 5G–H).

The flow cytometry findings were corroborated by MMP staining and subsequently fluorescence visualization. During a 24-hour incubation period, the combination of 20 μg/mL of COEtOAc with 6 μmol/L of sorafenib in HCT116 and 30 μg/mL of CODCM with 2 μmol/L of sorafenib in HepG2, exhibited apoptosis concurrent with a decrease in MMP levels compared to individual treatments. Furthermore, fluorescence microscopy employing H2DCFDA staining demonstrated an increase in ROS formation following the combination treatment (Figs. 6 and 7). These collective findings suggest that the lowest concentration of *C. odollam* fruit extracts, whether COEtOAc or CODCM, in combination with sorafenib at concentrations below their respective IC_{50} values, exhibits an anticancer effect via a mitochondrial-dependent apoptosis pathway. Notably, this mechanism is associated with ROS formation in both HCT116 and HepG2 cells.

3.4. Western blotting assessed levels of SOD2 and catalase following treatment with C. odollam fruit extracts combined with sorafenib on HCT116 and HepG2 cells

The mechanism underlying apoptosis following the combination treatment of COEtOAc or CODCM with sorafenib, was investigated herein, with a focus on enhanced oxidative stress. Elevated levels of ROS formation were evaluated as indicative of this process.

It is noted that disruption of the equilibrium of antioxidant enzymes responsible for scavenging ROS formation augmented cancer cells' response to chemotherapy, ultimately exacerbating the cellular damage inflicted upon them (Azzolin et al., 2016). The present study found a significant decrease in the level of SOD2 and catalase protein expression following combination treatment compared to individual treatments (Fig. 8A–F). The original uncropped western blots were shown in Fig. S2. These findings corroborate the proposition that oxidative stress amplifies the

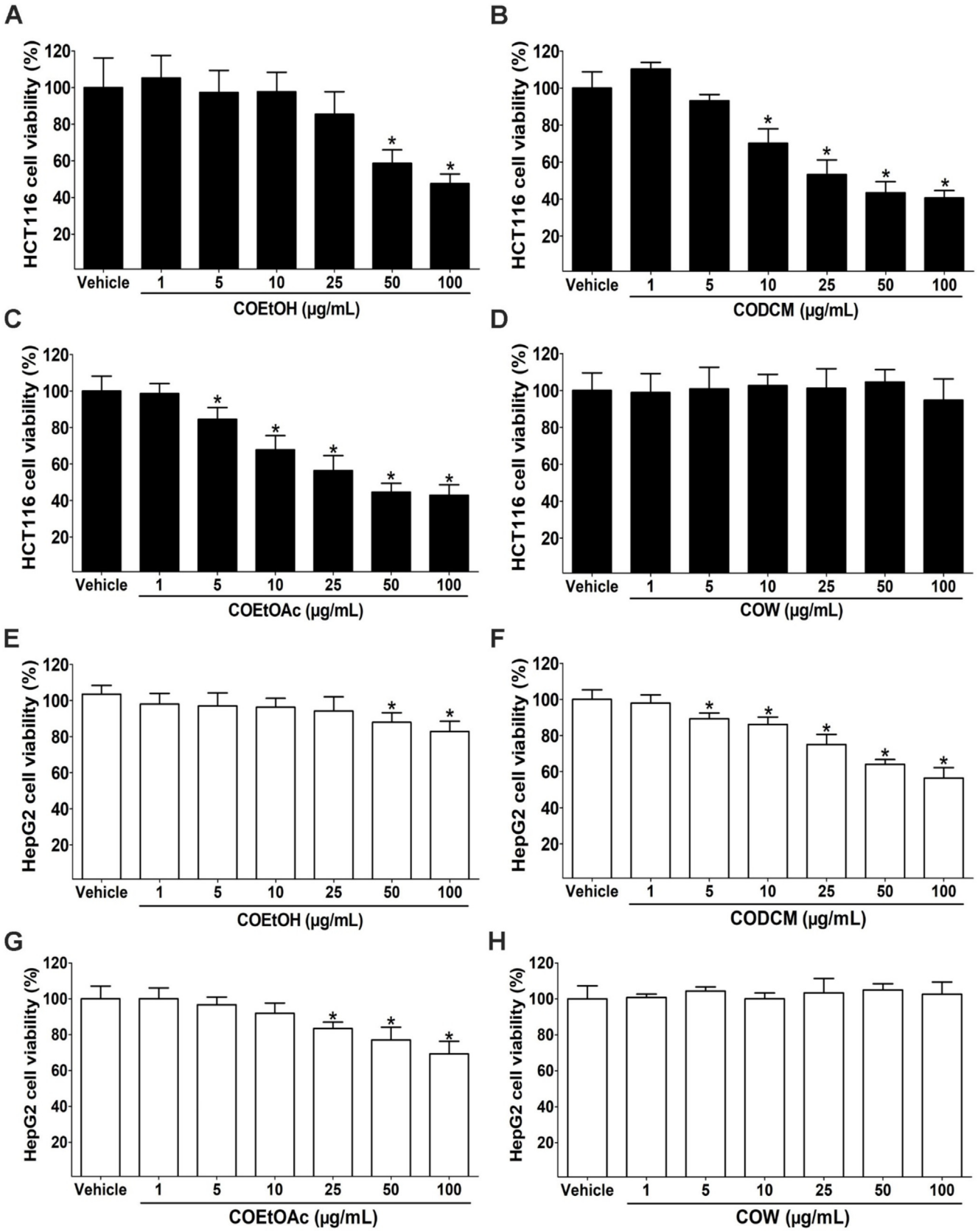

Fig. 2. Cytotoxicity of extracts from *C. odollam* fruits against HCT116 and HepG2 cells was assessed after 24 h of incubation using MTT technique to determine cell viability. (A–D) Demonstrating percentage of cell viability for HCT116 cells treated with COEtOH, CODCM, COEtOAc, and COW, respectively. (E–H) Showing percentage of cell viability for HepG2 cells treated with COEtOH, CODCM, COEtOAc, and COW, respectively. The vehicle control was represented by treatment with 0.8% DMSO. The data, presented as mean ± SD from at least three different experiments, were analyzed to investigate significant differences using One-way ANOVA with Tukey's HSD test. $^{*}P < 0.05$ *vs* vehicle control.

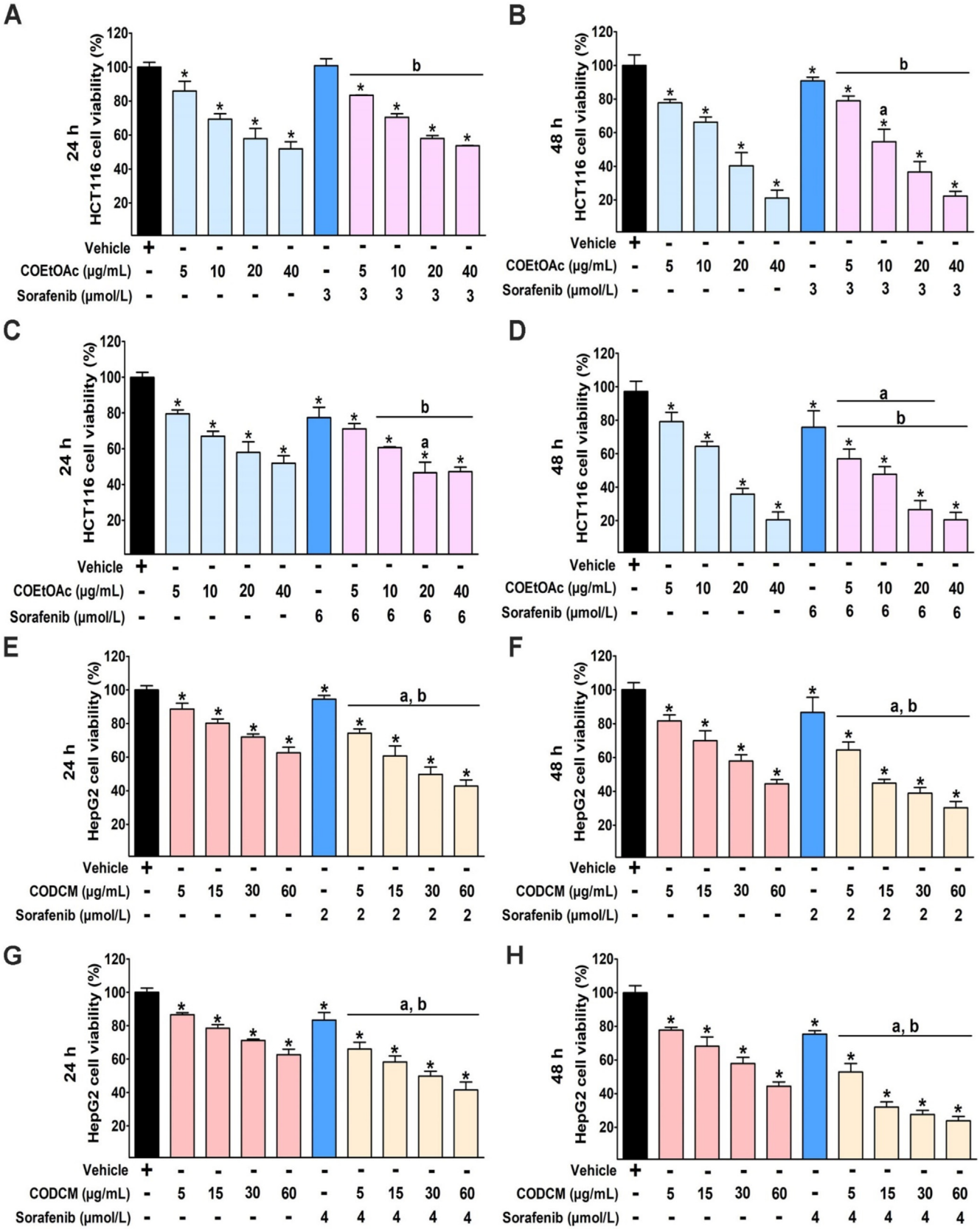

Fig. 3. Cytotoxicity of combination of COEtOAc or CODCM with sorafenib against HCT116 and HepG2 cells was assessed using MTT technique to measure cell viability. (A–D) Demonstrating percentage of cell viability in HCT116 cells treated with COEtOAc combined with sorafenib after 24 and 48 h of incubation, respectively. (E–H) Showing percentage of cell viability in HepG2 cells treated with CODCM combined with sorafenib after 24 and 48 h of incubation, respectively. The vehicle control was represented by treatment with 0.8% DMSO. The data, presented as mean ± SD from at least three different experiments, were analyzed to investigate significant differences using One-way ANOVA with Tukey's HSD test. $^{*}P < 0.05$ *vs* vehicle control, $^{a}P < 0.05$ *vs* a single COEtOAc or CODCM treatment at their respective doses, $^{b}P < 0.05$ *vs* a single sorafenib treatment.

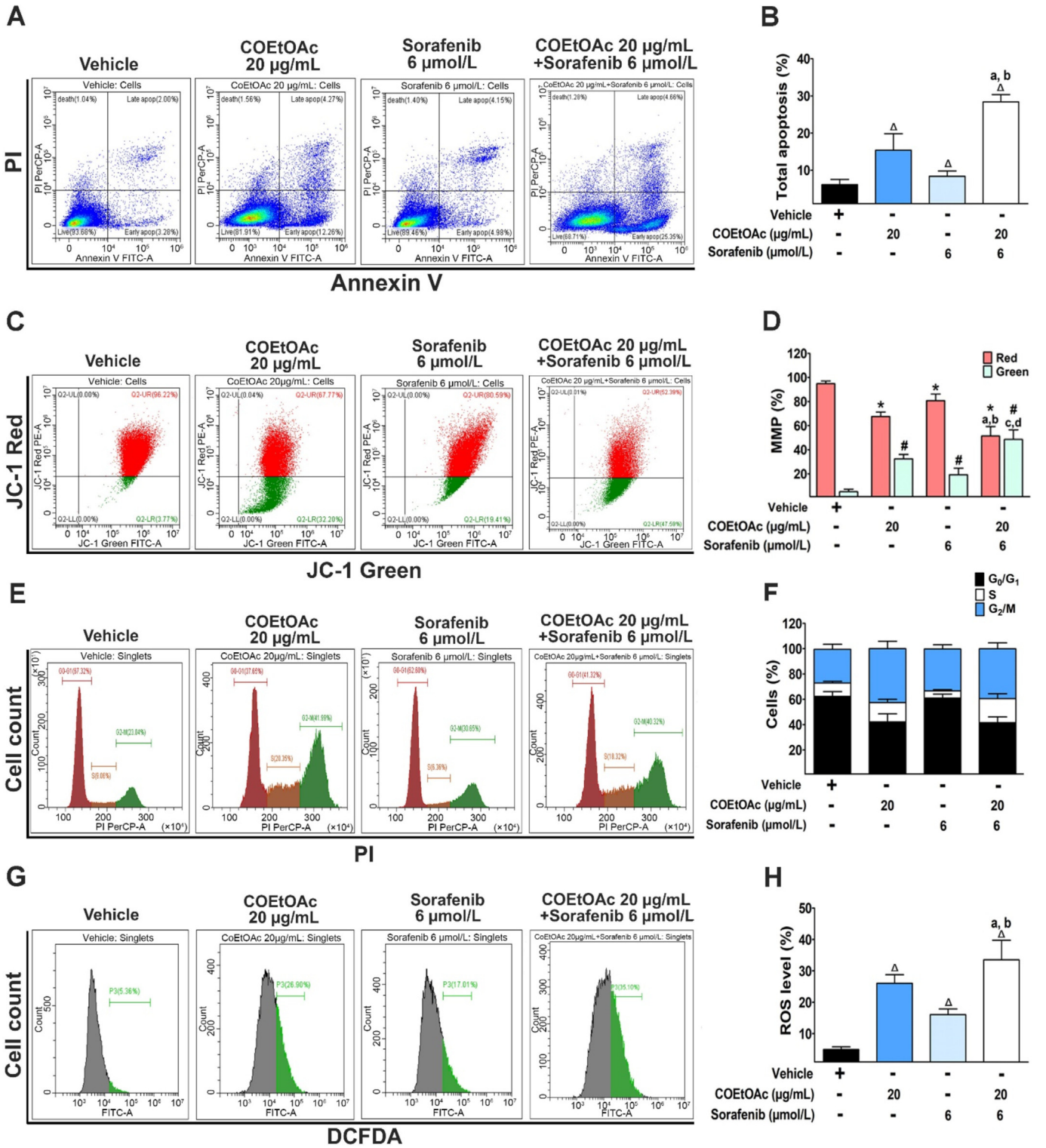

Fig. 4. Flow cytometric analysis was conducted to assess apoptotic effect, MMP, cell cycle distribution, and ROS levels following treatment with COEtOAc at 20 μg/mL combined with sorafenib at 6 μmol/L for 24 h in HCT116 cells. The data demonstrate: (A–B) apoptotic cells after double labeling with annexin V and PI, (C–D) MMP levels labeled with JC-1, (E–F) cell cycle distribution labeled with PI, and (G–H) ROS levels labeled with H2DCFDA. The vehicle control was represented by treatment with 0.8% DMSO. The data, presented as mean ± SD from at least three different experiments, were analyzed to investigate significant differences using One-way ANOVA with Tukey's HSD test. $^{\Delta}P < 0.05$ *vs* vehicle control, $^{*}P < 0.05$ *vs* vehicle control (red), $^{\#}P < 0.05$ *vs* vehicle control (green), $^{a}P < 0.05$ *vs* a single COEtOAc treatment, $^{b}P < 0.05$ *vs* a single sorafenib treatment.

responsiveness of cancer cells to the combined therapeutic approach using *C. odollam* fruit extracts, whether COEtOAc or CODCM, in conjunction with sorafenib in both HCT116 and HepG2 cells. Additionally, assessment of cytotoxicity demonstrated that the IC_{50} values [(125.16 ± 13.94) μg/mL for COEtOAc and (218.55 ± 32.29) μg/mL for CODCM] for HFF-1 cells were approximately threefold higher than those observed for COEtOAc or CODCM in HCT116 and HepG2 cancer cells (Fig. 8G–H). This suggests the potential for safe utilization of these extract concentrations in normal cells.

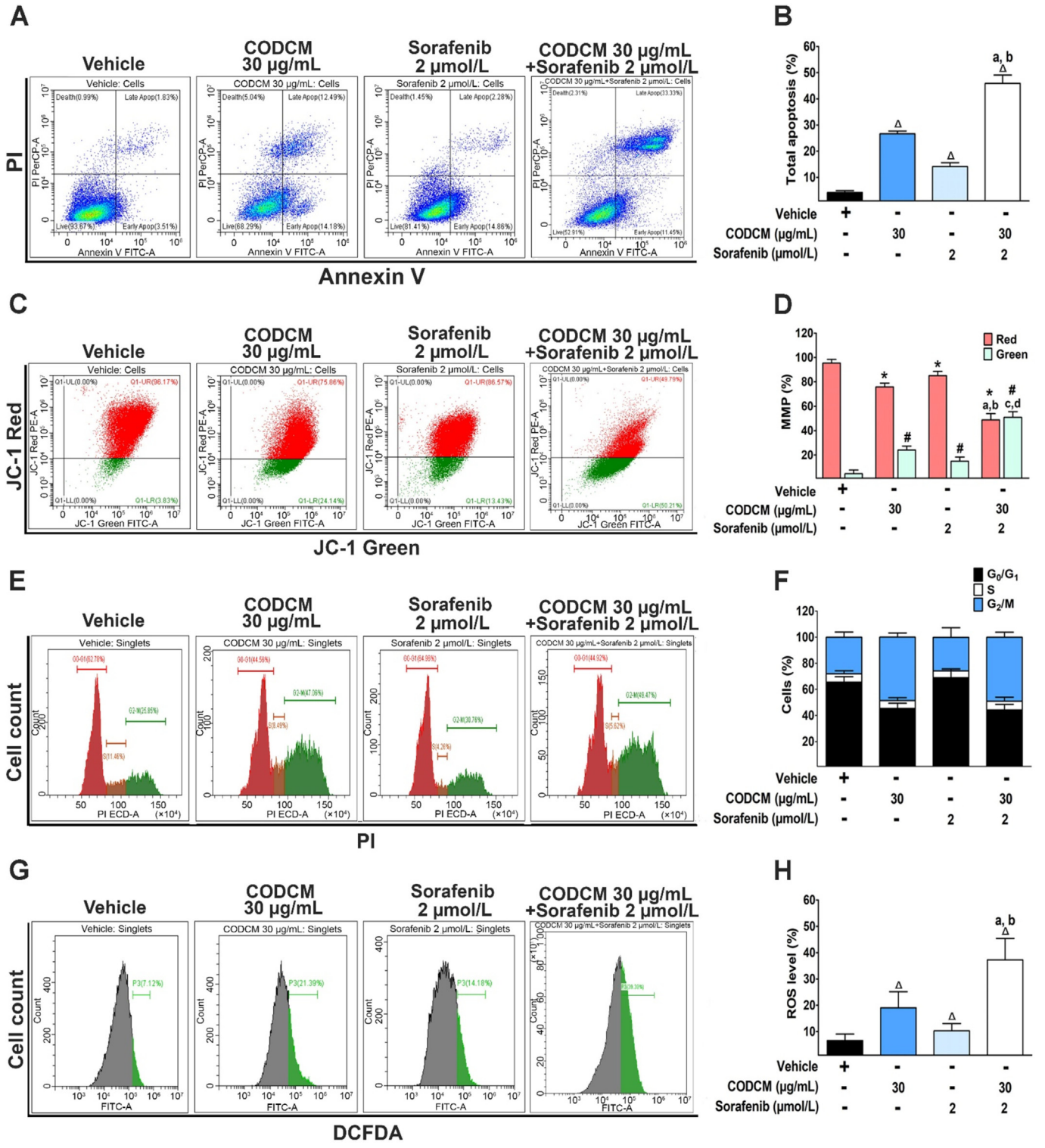

Fig. 5. Flow cytometric analysis was conducted to assess apoptotic effect, MMP, cell cycle distribution, and ROS levels following treatment with CODCM at 30 μg/mL combined with sorafenib at 2 μmol/L for 24 h in HepG2 cells. The data demonstrate: (A–B) apoptotic cells after double labeling with annexin V and PI, (C–D) MMP levels labeled with JC-1, (E–F) cell cycle distribution labeled with PI, and (G–H) ROS levels labeled with H2DCFDA. The vehicle control was represented by treatment with 0.8% DMSO. The data, presented as mean ± SD from at least three different experiments, were analyzed to investigate significant differences using One-way ANOVA with Tukey's HSD test. $^{\Delta}P < 0.05$ *vs* vehicle control, $^{*}P < 0.05$ *vs* vehicle control (red), $^{\#}P < 0.05$ *vs* vehicle control (green), $^{a}P < 0.05$ *vs* a single CODCM treatment, $^{b}P < 0.05$ *vs* a single sorafenib treatment.

4. Discussion

A crude ethanolic extract of *C. odollam* fruits was obtained through a solvent extraction method enhanced by ultrasonic assistance. The extraction process utilized three solvents: dichloromethane, ethyl acetate, and water, resulting in the separation of the COEtOH into three distinct fractions characterized by varying polarities: CODCM (non-polar fraction), COEtOAc (moderately

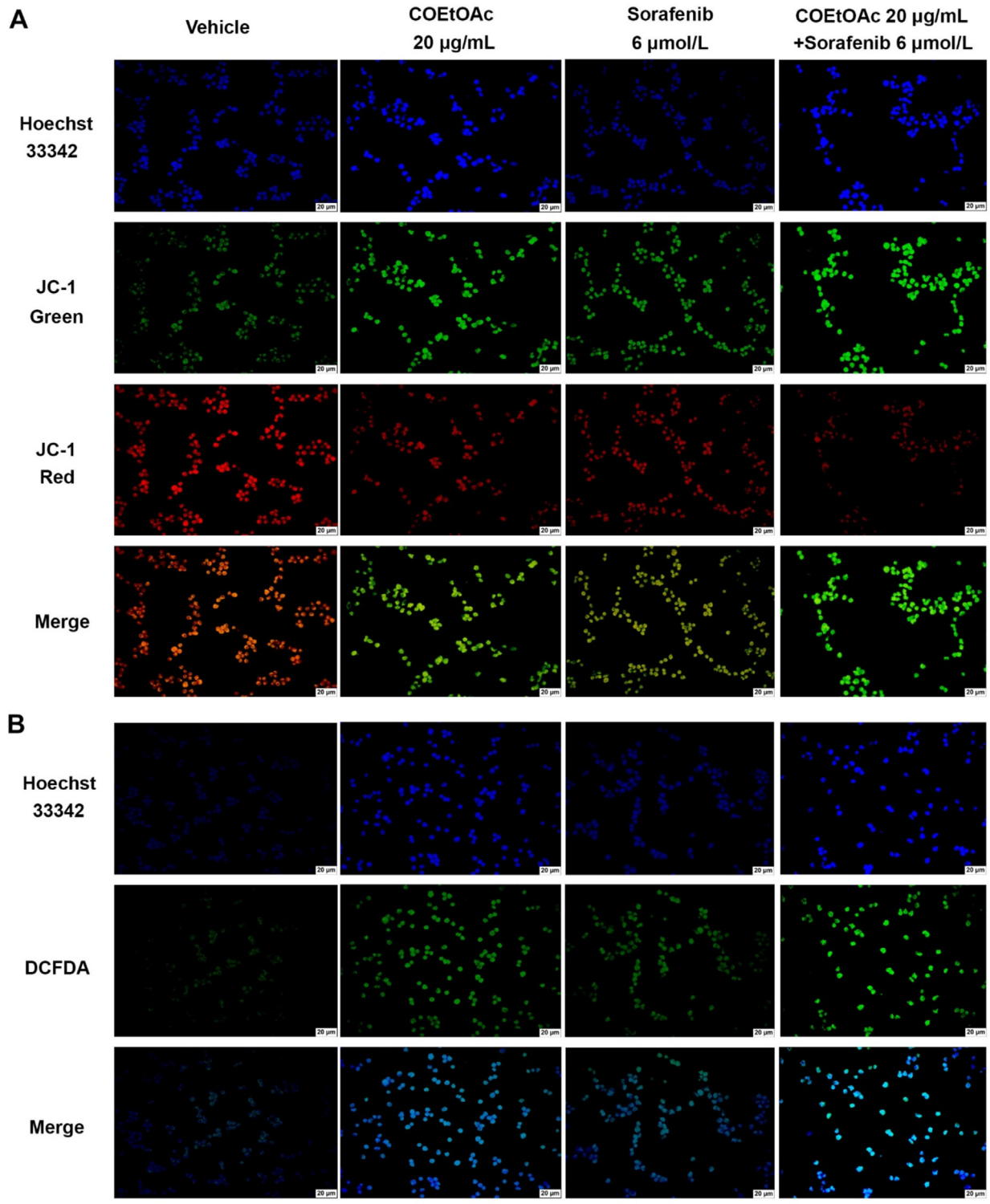

Fig. 6. Fluorescence images of MMP and ROS formation following treatment with COEtOAc at 20 μg/mL combined with sorafenib at 6 μmol/L for 24 h in HCT116 cells. The data demonstrates: (A) MMP, labeled with JC-1, and (B) ROS, labeled with H2DCFDA. Nuclear DNA was labeled with Hoechst 33342. The treatment with 0.8% DMSO served as vehicle control. Scale bar = 20 μm under × 20 magnification, visualized by fluorescence microscopy.

polar fraction), and COW (polar fraction). The phytochemical analysis of the four extracts revealed varying quantities of five groups of secondary metabolites: cardiac glycosides, triterpenoids, saponins, phenolics, and flavonoids (Fig. 1G). This composition aligns with our previous findings on *Calotropis gigantea* (L.) W. T. Aiton, a plant in the same family (Apocynaceae) as *C. odollam*, which was shown to contain cardiac glycosides, triterpenoids, phenolics, and flavonoids (Sawong et al., 2022; Winitchaikul et al., 2021). The COEtOAc fraction was rich in cardiac glycosides, phenolics, and flavonoids, with concentrations significantly higher than those in the other fractions by factors of 3.2–6.9, 5.9–21.1, and 6.0–20.7, respectively. Moreover, the CODCM fraction was abundant in triterpenoids and saponins, with levels significantly higher than those in the other fractions by factors of 1.4–2.0 and 1.5–2.9,

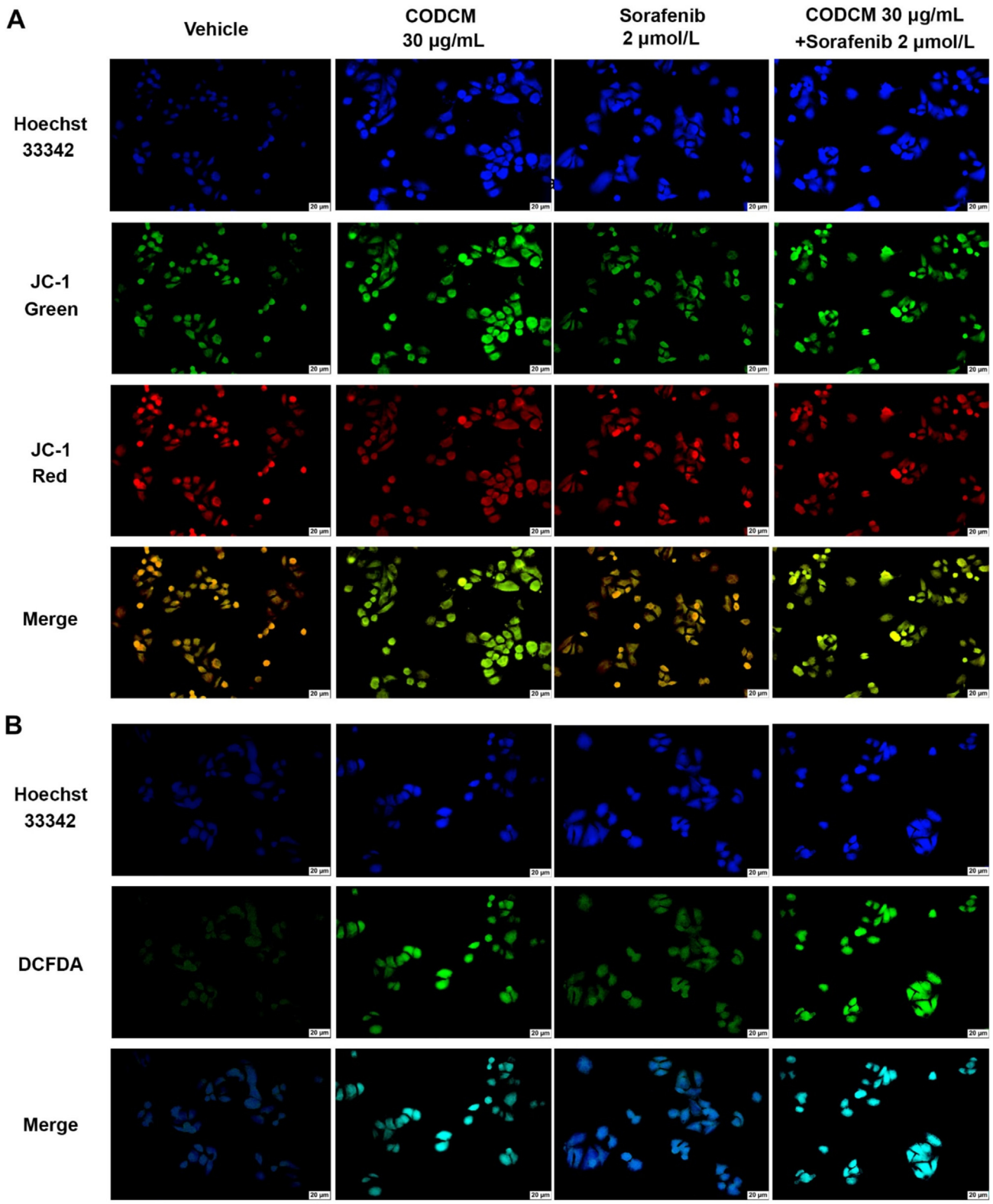

Fig. 7. Fluorescence images of MMP and ROS formation following treatment with CODCM at 30 μg/mL combined with sorafenib at 2 μmol/L for 24 h in HepG2 cells. The data demonstrates: (A) MMP, labeled with JC-1, and (B) ROS, labeled with H2DCFDA. Nuclear DNA was labelled Hoechst 33342. The treatment with 0.8% DMSO served as vehicle control. Scale bar = 20 μm under × 20 magnification, visualized by fluorescence microscopy.

respectively. These results indicated that liquid–liquid partition of COEtOH by using dichloromethane, ethyl acetate and water, could enrich different types of phytochemicals to each fraction which may involve in their anticancer activities. HPLC fingerprints (Fig. S1) of different *C. odollam* fractions showed different chemical composition. COEtOAc appeared to be a fraction containing more peaks numbers with high values of purity indexes than other fractions. The HPLC conditions employed in this study could be

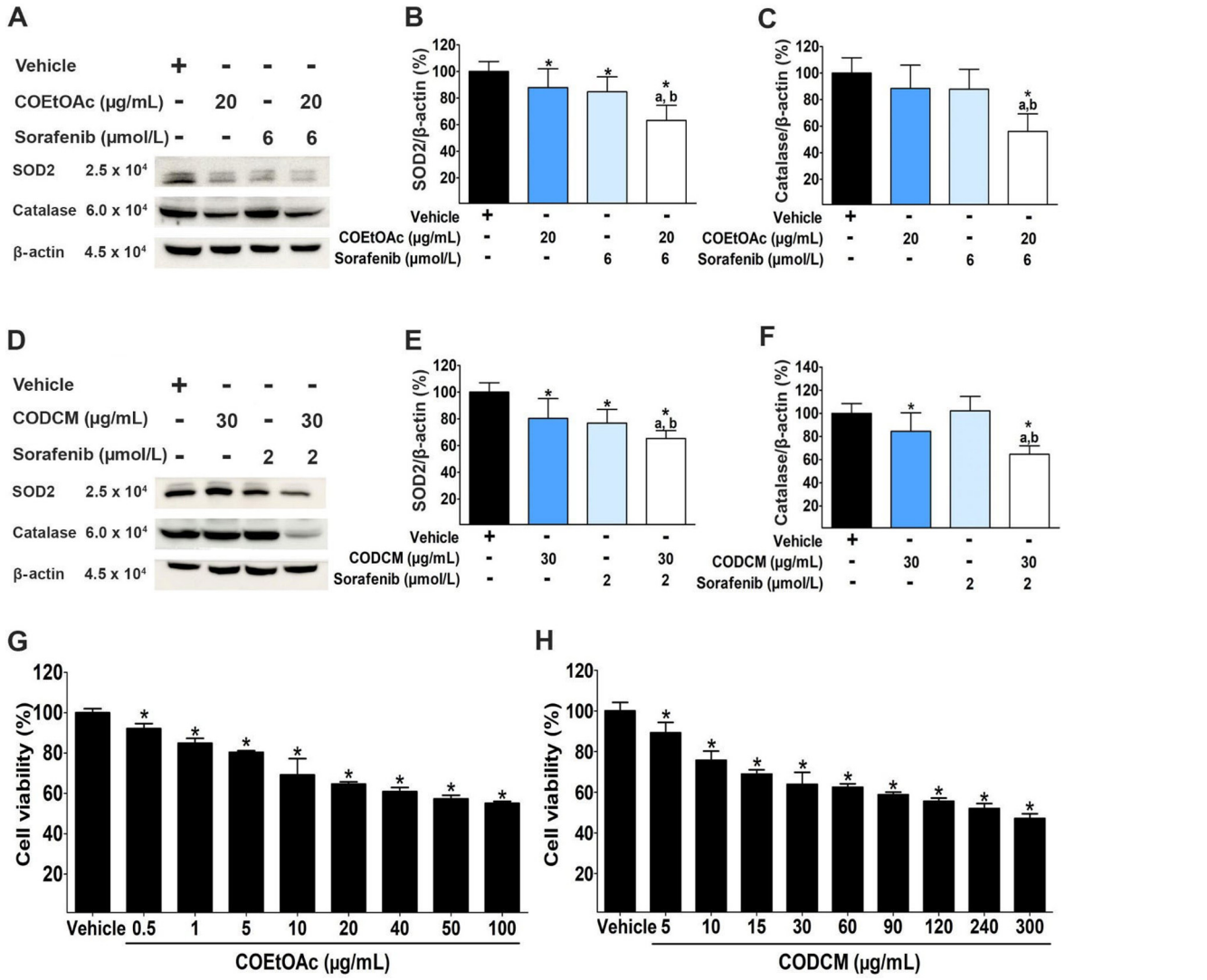

Fig. 8. Levels of protein SOD2 and catalase were assessed following treatment with COEtOAc or CODCM combined with sorafenib in HCT116 and HepG2 cells for 24 h. For HCT116 cells: (A–C) show representative western blot images and histograms depicting SOD2 and catalase levels following treatment with COEtOAc at 20 μg/mL combined with sorafenib at 6 μmol/L. For HepG2 cells: (D–F) show representative western blot images and histograms depicting SOD2 and catalase levels following treatment with CODCM at 30 μg/mL combined with sorafenib at 2 μmol/L. (G–H) Cell viability of HFF-1 cells following COEtOAc or CODCM treatment in 24 h. The vehicle control was represented by treatment with 0.8% DMSO. The data, presented as mean ± SD from at least three different experiments, were analyzed to investigate significant differences using One-way ANOVA with Tukey's HSD test. $^{*}P < 0.05$ *vs* vehicle control, $^{a}P < 0.05$ *vs* a single COEtOAc or CODCM treatment at their respective doses, $^{b}P < 0.05$ *vs* a single sorafenib treatment.

applicable for further development to use for quantitative analysis of some peaks for quality control purposes.

There have been few studies reporting on the mechanism of the anticancer potential of the extracts from *C. odollam*, while the widely discussed cardiotoxic effects have been demonstrated. This plant, belonging to Apocynaceae family, is known for its poisonous nature, primarily due to the rich presence of cardiac glycosides, specifically cardenolides, in the central kernel of its fruit, especially the COEtOAc fraction as shown in Fig. 1G. These compounds exhibit various biological and pharmacological activities, including the apoptotic induction against cancer cells. Unfortunately, these glycosides have been widely reported to be implicated in numerous cases of poisoning, both in suicides and homicides, and they are not easily detectable through digoxin assays (Menezes et al., 2018). Ingestion of seed kernels caused severe symptoms of cardiac glycoside-like cardiotoxic effects, cerberin was identified to generate these toxic effects (Rotella, Wong, Wong, & Graudins, 2020). Ingestion of extremely small amounts of the *C. odollam* kernel has been reported to result in death, with a lethal dose of 1.8 mg/kg in dogs and 3.8 mg/kg in cats (Menezes et al., 2018). In addition to their application in treating heart failure by inhibiting Na/K-ATPase activity, as reported with cardiac glycosides, such as digoxin, and cardenolides, which have a narrow therapeutic index, these compounds also induce apoptosis in cancer cells at low nanomolar dosages (Lu, Lui, Huang, Chang, & Lin, 2014; Zhou et al., 2019).

Few reports have demonstrated the potential anticancer activity of crude extracts from *C. odollam* in many cancer models (Gorantla, Vellekkatt, Nath, Anto & Lankalapalli, 2014; Hossan et al., 2019; Yunos, Osman, Jauri, Sallehudin, & Mutalip, 2020). Our present study demonstrated consistent results with these findings, showing that COEtOAc treatment in HCT116 cells and CODCM treatment in HepG2 cells, after a 24-hour incubation, had the lowest IC_{50} values among other extract fractions from *C. odollam* whole fruit. Furthermore, we reported the safe usage of COEtOAc and CODCM as they exhibited lower cytotoxicity in HFF-1 cells, with IC_{50} values approximately 2–3 times higher than those found in cancer cells. These findings not only verify the therapeutic poten-

tial of the extract at low concentrations, minimizing toxic effects on normal cells, but also demonstrate that combining it with sorafenib enhances the effectiveness of anticancer therapy.

More than 20 cardenolides from the Apocynaceae family exhibit selective anticancer activity. The potent anticancer potential of cardiac glycosides involves the expression of pro-apoptotic molecules and induces cell cycle arrest following an increase intracellular calcium influx (El-Seedi et al., 2019; McConkey, Lin, Nutt, Ozel, & Newman, 2000; Riganti et al., 2009). Deslanoside inhibited cancer cell viability by apoptosis induction with low cytotoxic effect on normal cells, has been found to involve the expression of genes in oncogenic and tumor suppressive functions (Liu et al., 2021). The anticancer activity of cardenolides is primarily mediated through the inhibition of the Na/K-ATPase-dependent pathway (Geng et al., 2020). Inhibiting the activity and inducing conformational changes of Na/K-ATPase by binding to specific isoforms expressed in cancer cells, cardenolides exert important roles in targeting growth, motility, and apoptosis in cancer cells (Wen et al., 2016). Cerberin, isolated from the fruit kernel of *C. odollam*, exhibited cytotoxicity through the inhibition of Na/K-ATPase. This inhibition reduced intracellular Na^+ and elevated Ca^{2+} levels (Hossan et al., 2019). The apoptotic activity of 17βH-neriifolin, isolated from *C. odollam* leaves, showed a similar effect to that of ouabain and paclitaxel through the inhibition of Na/K-ATPase activity (Yunos, Osman, Jauri, Sallehudin, & Mutalip, 2020).

Numerous reports have demonstrated that the anticancer activity of cardiac glycoside components in herbal plants is mechanistically linked to ROS generation (Ajibare et al., 2022; Hossan et al., 2019; Sikdar, Mukherjee, Ghosh, & Khuda-Bukhsh, 2014). Inhibition of the activity of Na/K-ATPase by cardiac glycoside ouabain in HT-29 cells leads to elevated ROS levels, leading to apoptosis in cancer cells, without significant effects on normal cells (Fujii et al., 2018). In addition to digoxin, cardiac glycosides like proscillaridin A and lanatoside C, which have received approval for clinical use by the Food and Drug Administration, the European Medicines Agency, and other regulatory agencies, have been found to promote apoptosis through increased ROS formation in uterine leiomyosarcoma (Nagao et al., 2023). The anticancer activity of cerberin extracts from *C. odollam* has shown that ROS formation is associated with its mechanism of action, subsequently causing DNA double-strand breaks in cancer cells (Hou, Shang, Meng, & Lou, 2021). Therefore, ROS formation following the administration of cardiac glycosides plays an important role as mediator of apoptosis in anticancer applications.

Other mechanisms of potential anticancer activity of cardiac glycoside have been studied. Oleandrin, cardiac glycoside extracted from leaves of *Nerium oleander*, exerted the anticancer effect via enhanced tumor destruction by immunologic process activation (Li et al., 2021a). In addition, triterpenoids found in *C. odollam*, have been suggested to induce apoptosis both independently and in combination with a Toll-like receptor-9 (TLR9) agonist, reducing the viabilities of cancer cells both *in vitro* and *in vivo* (Ru et al., 2023). Triterpenoids derived from the Cucurbitaceae plant induced TLR4-triggering pyroptosis cell death, which consequently enhanced mitochondrial ROS production, thereby targeting cancer cells while being safe for normal cells (Yuan et al., 2021). Additionally, saponins from *Anemarrhena asphodeloides* Bunge induced cancer cell death through lipid peroxidation caused by ROS generation (Zhou et al., 2023). Polyphenolic curcumin from rhizome of the *Curcuma longa* L. inhibited breast cancer cell growth by activating ROS-mediated YAP-JNK phosphorylation pathway (Wang et al., 2019). Polyphenol compounds isolated from *Agrimonia pilosa ledeb* induced cancer cell death through the accumulation of ROS by inhibiting the PI3K/AKT/mTOR pathway, consequently regulating the glycolytic pathway in cancer cells by suppressing hypoxia-inducible factor 1-α expression (Zhu et al., 2022). Moreover, flavonoids from lotus leaves promoted cancer cell death through ROS accumulation, inducing oxidative stress activity and activating the p38 mitogen-activated protein kinase (MAPK) pathway (Jia, Zhang, Xu, Yao, Wei, 2021). Flavonoids extracted from dried leaf of *Artemisia argyi* Levl. et Vant. induced cancer cell death by increasing ROS production, which regulates the MAPK signaling pathway and the activator of transcription 3 (STAT3)/NF-κB signaling pathway (Liu et al., 2024). The proposed anticancer properties of *C. odollam* fruit extract is attributed to its predominant phytochemical constituents, with the mechanism primarily centered on the generation of ROS.

An increase in ROS production can lead to cell damage through lipid peroxidation (Silva et al., 2017). The inhibition of Na/K-ATPase in cancer cells triggers the activation of the Ras-Raf-MEK-ERK1/2 signaling pathway, thereby enhancing ROS-mediated apoptosis (Trenti et al., 2014). The overall imbalance between antioxidant enzyme activity and level of ROS, where ROS levels dominate over antioxidants, leads to the induction of apoptosis in cancer cells (Kang, Hong, Choi, & Lee, 2016; Arumugam et al., 2016). Increased ROS formation is responsible for the initiation of mitochondrial damage during the early apoptotic stage in cancer cells following the anticancer treatments (Mondal & Bennett, 2016). SOD2, located in the mitochondrial matrix, is recognized as a tumor suppressor gene that regulates the proliferation of cancer cells. Increasing oxidative stress through elevated levels of superoxide anions while reducing SOD2 levels enhances the cytotoxic effects and induces apoptosis in cancer cells following chemotherapy (Arumugam et al., 2016; Azzolin et al., 2016). Depletion of SOD2 and catalase levels can exacerbate oxidative stress-induced apoptosis in cancer cells (Jia et al., 2021).

Currently, the combination of plant-based or edible food extracts with chemotherapy drugs has shown greater anticancer potential than drug treatment alone, with minimal side effects on normal cells (Cianciosi et al., 2022; Cianciosi et al., 2023, Cianciosi et al., 2024). In addition, the anticancer effect of this combination was associated with profound increased ROS production, suppression of antioxidant enzyme, and downregulation of cell proliferation signaling pathway proteins, suggesting its potential as adjuvant cancer therapy (Afrin et al., 2018) and enhancing the sensitivity of drug-resistant cell lines to chemotherapy (Wei et al., 2022). Combining cardiac glycosides with anticancer drugs offers potential therapeutic interventions that are less cytotoxic to normal cells (Zhang et al., 2021b; Liu et al., 2020).

Sorafenib targets cell surface receptor tyrosine kinases, including platelet-derived growth factor receptor (PDGFR-β), vascular endothelial growth factor receptor (VEGFR 2), and hepatocyte factor receptor (c-KIT). It inhibits the activation of MAPK pathway, which consists of Raf, MEK (MAPK kinase) and extracellular signal-regulated kinase (ERK), thereby suppressing cancer cell proliferation by inhibiting the downstream expression of Raf serine/threonine kinase isoforms [A-Raf, B-Raf and Raf1 (or C-Raf)] (Tang et al., 2020; Wilhelm et al., 2006). However, several mechanisms of acquired drug resistance contribute to poor efficacy of sorafenib within the six months after treatment (She et al., 2024). These mechanisms include adenosine triphosphate (ATP) binding box (ABC) transporters, which reduce the chemotherapy effectiveness by expelling drugs from cancer cells, thereby modifying the regulated cell death pathways (Sun et al., 2022). In resistance cells, ROS levels and MMP are reduced, along with lower mitochondria and mitochondrial DNA levels, suggesting a diminished oxygen consumption rate in mitochondrial respiratory capacity (Vishnoi et al., 2022; Xu et al., 2021). Additionally, sorafenib-resistant HCC cells exhibit decreased ROS levels and ferroptosis inhibition, which are associated with resistance (Hu et al., 2023). A critical driver of sorafenib resistance in HCC is the activation of phosphoglycerate dehydrogenase (PHGDH), the key enzyme

in serine synthesis pathway, which generates antioxidants and α-ketoglutarate to overcome ROS production by sorafenib (Wei et al., 2019).

To overcome resistance to sorafenib and improve cancer treatment efficacy, novel combination strategies involving sorafenib and cytotoxic agents have been studied (Roskoski Jr, 2024). Specifically, combining sorafenib with anticancer agents, such as plant extracts or molecules from the apoptotic protein family that exhibit lower cytotoxicity toward normal cells, has been shown to increase the cytotoxic potential of sorafenib and improve treatment outcomes compared to control and single-dose treatments (He et al., 2023; Hussain, Meena, & Sinha, 2023; Kim et al., 2017; Şirin, Elmas, Secme, & Dodurga, 2020; Üremiş, Üremiş, & Türköz, 2023).

Only a few studies have reported the combined effects of cardiac glycosides and their synergistic enhancement of sorafenib's anticancer activity (Yang et al., 2021; Xiao et al., 2017). Our study focused on the cytotoxic effect of combining sorafenib with *C. odollam* fruit extracts in cancer cells. This combination demonstrated complementary anticancer effect, suggesting that *C. odollam* could sensitize HCT116 and HepG2 cells to sorafenib-induced apoptosis. Several studies have shown that the sensitivity of cancer cells to sorafenib is enhanced by combining it with various medicinal plant extracts (Chen, Chiang, & Hsu, 2019; Dai et al., 2018; Ghanem et al., 2023; Li et al., 2024; Omar, Tolba, Hung, & Al-Tel, 2016; Üremiş Üremiş, & Türköz, 2023; Wei et al., 2022). Our findings suggest that increased ROS formation is the primary mechanism responsible for apoptosis induction when sorafenib is used in conjunction with the extract in HCT116 and HepG2 cells. The cytotoxic mechanism involving increased ROS formation due to the combination of sorafenib with *C. odollam* fruit extracts in cancer cells has not been previously explored. However, numerous studies have underscored the critical role of ROS in sensitizing cancer cells to apoptosis when sorafenib is combined with other anticancer agents (Kuo et al., 2022; Li et al., 2022; Mondal & Bennett, 2016; Sun et al., 2021; Yao, Zhao, Yin, Wang, & Gao, 2020; Zheng et al., 2022).

Notably, ROS production was significantly induced by mitochondrial damage, leading to ATP depletion (Zhang et al., 2021a). This mitochondrial disruption, coupled with the activation of mitophagy, further sensitized cancer cells, including those resistant to sorafenib (Zhou et al., 2023). Additionally, oxidative stress, along with ROS accumulation, has been demonstrated as a contributor to sensitizing cancer cells to sorafenib (Wei et al., 2019). Increased ROS production, coupled with a reduction in redox capacity, has been suggested as a mechanism to sensitize sorafenib-resistant HCC. This effect is linked to the upregulation of PHGDH in the serine synthesis pathway in HCC (Wei et al., 2019). There are limited studies on the effects of plant extracts in improving sorafenib resistance in cancer cells. For example, the combination of 20(*R*)-ginsenoside Rg3 from red ginseng with the antimalarial drug artesunate demonstrated a synergistic effect in inducing apoptosis. This effect was mediated by increased ROS generation, which contributed to the inhibition of Src/STAT3 signaling and improved the response of HepG2 cells to sorafenib-resistant treatment (Chen et al., 2022).

Consistent with previous reports, the anticancer mechanism of the combination treatment primarily involved the induction of apoptosis. However, the interaction between apoptosis and autophagy in anticancer effects is complex and multifaceted. While some studies have demonstrated a positive correlation between the two processes, others suggest that autophagy can negatively modulate apoptosis, thereby protecting cells from death under certain conditions (Kang et al., 2022; Rong et al., 2020; Wang et al., 2022a; Zhou, Jiang, Chen, Wu, & Zhang, 2020; Zhu et al., 2021). The relationship between apoptosis and autophagy in cancer treatment, particularly when targeted by plant extracts, remains controversial. For example, periplocymarin, isolated from the dried root bark of *Periploca sepium* Bunge, and known for its richness in cardiac glycosides, has been shown to decrease ATP production in both glycolytic and mitochondrial pathways by inhibiting the Na/K-ATPase pump. This inhibition leads to apoptosis in cancer cells. Notably, the inhibition of autophagy sensitizes cancer cells to apoptosis induced by periplocymarin (Hao et al., 2023). However, the relationship between apoptosis and autophagy in cancer treatment, particularly when sorafenib is combined with other agents, also remains controversial. Studies have shown that autophagy levels increase when sorafenib is combined with other drugs to induce apoptosis in cancer cells. For example, combinations like doxercalciferol with carnosic acid (Wu et al., 2020), carnosic acid (Wang et al., 2020), artesunate (Ma et al., 2024), or epalrestat, (Geng, Jin, Li, Zhu, & Bai, 2020) with sorafenib have been shown to enhance its cytotoxic effects by inducing both apoptosis and autophagy. On the other hand, the combination of sorafenib with escin (Hussain, Singh, Meena, Sinha, & Luqman, 2023, 2024) inhibits autophagy and induces late-stage apoptosis. Therefore, future studies should focus on thoroughly investigating the potential of *C. odollam* extract to enhance sorafenib's effects on anticancer pathways.

Induction of ROS-mediated apoptosis in cancer cells is closely linked to cellular ATP production, as demonstrated in multiple studies (Martínez-Torres et al., 2020; Shen, Zhang, Wang, Zhang, & Gong, 2014; Wiczk, Hofman, Konopa, & Herman-Antosiewicz, 2012). Mitochondrial dysfunction, which disrupts oxidative phosphorylation (OXPHOS), leads to ATP depletion and subsequently triggers apoptosis in cancer cells (Feng et al., 2019; Song, Ham, Park, Song, & Lim, 2024). The activation of AMPK and the depletion of ATP levels following mitochondrial dysfunction have been associated with increased ROS formation, culminating in apoptosis (Kim et al., 2019). Notably, sorafenib has been reported to decrease OXPHOS activity, resulting in the collapse of MMP and reduced ATP synthesis. The irregular morphology of mitochondria interferes with ROS homeostasis, potentially resulting in lipid peroxidation. This process may enhance the cytotoxic effects of sorafenib, particularly when used in conjunction with other anticancer therapies (Bandy et al., 2023; Li et al., 2021b; Liu, Wang, Meng, Lu, & Peng, 2023). The anticancer efficacy of sorafenib has been extensively studied in combination with various agents, often implicating glycolysis as a central mechanism. The antiglycolytic agent 2-deoxyglucose, in combination with sorafenib, significantly inhibited sorafenib-resistant cells by reducing ATP levels and attenuating glycolysis and OXPHOS, suggesting that suppression of glycolytic flux is a key mechanism enhancing the efficacy of sorafenib in treating sorafenib-resistant cancer (Reyes, Wani, Ghoshal, Jacob, & Motiwala, 2017). Furthermore, the reduction in basal mitochondrial oxygen consumption rates, specifically targeting OXPHOS-related ATP production, also completely depletes glycolytic reserves in cancer cells when sorafenib is combined with anticancer agents (Zhang et al., 2018). Depletion of intracellular ATP, extracellular *L*-lactate levels, extracellular acidification rates, and oxygen consumption rates, collectively promote enhanced apoptosis effect of sorafenib in cancer cells (Wang et al., 2015). Despite these advances, the therapeutic potential and underlying molecular mechanisms of combining sorafenib with *C. odollam* fruit extracts in cancer cells remain largely unexplored and warrant further investigation.

Our study demonstrated that ROS generation primarily enhanced apoptosis when *C. odollam* fruit extract was combined with sorafenib, synergizing the response in HCT116 and HepG2 cells. However, there are some limitations to this study. Further testing in various types of cancer cells is necessary to confirm the therapeutic anticancer properties and to determine the appropriate therapeutic dosage for both cancer and normal cells. Additionally, to elucidate the clinical applicability of this combination

regimen, it is essential to use cancer resistance models. Future experiments should also examine the relationship between apoptosis and autophagy to gain a deeper understanding of the underlying mechanisms. Additionally, animal models should be employed to explore the systemic anticancer efficacy, ensuring its potential future use as a medicinal agent, either as a standalone treatment or in combination with other anticancer drugs.

5. Conclusion

In conclusion, we advocate for a novel therapeutic approach that integrates *C. odollam* fruit extracts with sorafenib, which may provide considerable benefits in cancer treatment. This strategy has the potential to reduce the adverse effects associated with existing anticancer therapies while simultaneously improving overall treatment effectiveness, thereby establishing a foundation for future clinical use. Nonetheless, it is crucial to consider the possible toxicity linked to the cardiac glycosides found in *C. odollam*. Further research is required to validate the safety of these extracts for clinical applications. Future directions should include the extraction and characterization of active constituents, particularly cardiac glycosides, which possess considerable promise for improving the therapeutic efficacy of anticancer compounds sourced from toxic plants.

CRediT authorship contribution statement

Supawadee Parhira: Conceptualization, Data curation, Formal analysis, Funding acquisition, Investigation, Methodology, Software, Validation, Visualization, Writing – original draft, Writing – review & editing. **Orakot Simanurak:** Formal analysis, Investigation, Methodology, Visualization, Writing – original draft, Writing – review & editing. **Khemmachat Pansooksan:** Investigation, Methodology, Writing – review & editing. **Julintorn Somran:** Writing – review & editing. **Apirath Wangteeraprasert:** Writing – review & editing. **Zhihong Jiang:** Methodology, Writing – review & editing. **Liping Bai:** Methodology, Writing – review & editing. **Pranee Nangngam:** Methodology, Visualization, Writing – review & editing. **Dumrongsak Pekthong:** Data curation, Formal analysis, Investigation, Methodology, Software, Validation, Visualization, Writing – original draft, Writing – review & editing. **Piyarat Srisawang:** Conceptualization, Data curation, Formal analysis, Funding acquisition, Investigation, Methodology, Software, Validation, Visualization, Writing – original draft, Writing – review & editing.

Declaration of competing interest

The authors declare that they have no known competing financial interests or personal relationships that could have appeared to influence the work reported in this paper.

Acknowledgements

This work was supported by the National Science Research and Innovation Fund (NSRF) of Thailand (No. R2566B047), the Agricultural Research Development Agency (Public Organization), Thailand (No. CRP6505030030), the Global and Frontier Research University Fund, Naresuan University, Thailand (No. R2567C003), and the Science and Technology Development Fund, Macau SAR [No. 006/2023/SKL (MUST)]. The funders had no role in study design, data collection, and analysis, decision to publish, or preparation of the manuscript.

This manuscript has undergone proofreading and editing by Mr. Olalekan Israel Aiikulola, who serves as a Lecturer in Special Knowledge and Abilities at the Faculty of Medical Science, Naresuan University, Thailand.

Appendix A. Supplementary material

Supplementary data to this article can be found online at https://doi.org/10.1016/j.chmed.2024.11.007.

References

Afrin, S., Giampieri, F., Forbes-Hernández, T. Y., Gasparrini, M., Amici, A., Cianciosi, D., ... Battino, M. (2018). Manuka honey synergistically enhances the chemopreventive effect of 5-fluorouracil on human colon cancer cells by inducing oxidative stress and apoptosis, altering metabolic phenotypes and suppressing metastasis ability. *Free Radical Biology and Medicine, 126*, 41–54.

Ajibare, A. C., Ebuehi, O. A. T., Adisa, R. A., Sofidiya, M. O., Olugbuyiro, J. A. O., Akinyede, K. A., ... Ekpo, O. E. (2022). Fractions of *Hoslundia opposita* Vahl and hoslundin induced apoptosis in human cancer cells *via* mitochondrial-dependent reactive oxygen species (ROS) generation. *Biomedicine & Pharmacotherapy, 153*, 113475.

Alsulaimany, M., El-Adl, K., Aljohani, A. K. B., Alharbi, H. Y., Alatawi, O. M., Aljohani, M. S., ... Mohamed, A. A. (2023). Design, synthesis, docking, ADMET and anticancer evaluations of *N*-alkyl substituted iodoquinazoline derivatives as dual VEGFR-2 and EGFR inhibitors. *RSC Advances, 13*(51), 36301–36321.

Arumugam, A., Subramani, R., Nandy, S., Powell, S., Velazquez, M., Orozco, A., ... Lakshmanaswamy, R. (2016). Desacetyl nimbinene inhibits breast cancer growth and metastasis through reactive oxygen species mediated mechanisms. *Tumor Biology, 37*(5), 6527–6537.

Azzolin, V. F., Cadoná, F. C., Machado, A. K., Berto, M. D., Barbisan, F., Dornelles, E. B., ... da Cruz, I. B. M. (2016). Superoxide-hydrogen peroxide imbalance interferes with colorectal cancer cells viability, proliferation and oxaliplatin response. *Toxicology in Vitro, 32*, 8–15.

Bandy, R., Shahi, S., Quagraine, N., Shahbazi Nia, S., Howlader, M. S. I., Srivenugopal, K., ... German, N. A. (2023). Mechanistic aspects of biphenyl urea-based analogues in triple-negative breast cancer cell lines. *ACS Pharmacology & Translational Science, 7*(1), 120–136.

Chan, E. W. C., Wong, S. K., & Chan, H. T. (2016). Apocynaceae species with antiproliferative and/or antiplasmodial properties: A review of ten Genera. *Journal of Integrative Medicine, 14*(4), 269–284.

Chantrapromma, S., Usman, A., Fun, H. K., Laphookhieo, S., Karalai, C., Rat-a-pa, Y., & Chantrapromma, K. (2003). Bis[14β-hydroxy-3β-*O*-(*L*-thevetosyl)-5β-card-20(22)-enolide] methanol solvate monohydrate and 3β-*O*-(*L*-2'-*o*-acetylthevetosyl)-14β-hydroxy-5β-card-20(22)-enolide. *Acta Crystallographica Section C Crystal Structure Communications, 59*(2), o68–o70.

Chen, J. H., Chiang, I. T., & Hsu, F. T. (2019). Protein kinase B inactivation is associated with magnolol-enhanced therapeutic efficacy of sorafenib in hepatocellular carcinoma *in vitro* and *in vivo*. *Cancers, 12*(1), 87.

Chen, Y. J., Wu, J. Y., Deng, Y. Y., Wu, Y., Wang, X. Q., Li, A. S., ... Liang, C. (2022). Ginsenoside Rg3 in combination with artesunate overcomes sorafenib resistance in hepatoma cell and mouse models. *Journal of Ginseng Research, 46*(3), 418–425.

Cheng, A. L., Qin, S., Ikeda, M., Galle, P. R., Ducreux, M., Kim, T. Y., ... Finn, R. S. (2022). Updated efficacy and safety data from IMbrave150: Atezolizumab plus bevacizumab *vs.* sorafenib for unresectable hepatocellular carcinoma. *Journal of Hepatology, 76*(4), 862–873.

Cianciosi, D., Armas Diaz, Y., Alvarez-Suarez, J. M., Chen, X., Zhang, D., Martínez López, N. M., ... Giampieri, F. (2023). Can the phenolic compounds of Manuka honey chemosensitize colon cancer stem cells? A deep insight into the effect on chemoresistance and self-renewal. *Food & Chemistry, 427*, 136684.

Cianciosi, D., Forbes-Hernandez, T., Armas Diaz, Y., Elexpuru-Zabaleta, M., Quiles, J. L., Battino, M., & Giampieri, F. (2024). Manuka honey's anti-metastatic impact on colon cancer stem-like cells: Unveiling its effects on epithelial-mesenchymal transition, angiogenesis and telomere length. *Food & Function, 15*(13), 7200–7213.

Cianciosi, D., Forbes-Hernández, T. Y., Regolo, L., Alvarez-Suarez, J. M., Quinzi, D., Sargenti, A., ... Battino, M. (2022). Manuka honey in combination with 5-fluorouracil decreases physical parameters of colonspheres enriched with cancer stem-like cells and reduces their resistance to apoptosis. *Food Chemistry, 374*, 131753.

Dai, N., Ye, R., He, Q., Guo, P., Chen, H., & Zhang, Q. (2018). Capsaicin and sorafenib combination treatment exerts synergistic anti-hepatocellular carcinoma activity by suppressing EGFR and PI3K/Akt/mTOR signaling. *Oncology Reports, 40*(6), 3235–3248.

El-Seedi, H. R., Khalifa, S. A. M., Taher, E. A., Farag, M. A., Saeed, A., Gamal, M., ... Efferth, T. (2019). Cardenolides: Insights from chemical structure and pharmacological utility. *Pharmacological Research, 141*, 123–175.

Elwan, A., Abdallah, A. E., Mahdy, H. A., Dahab, M. A., Taghour, M. S., Elkaeed, E. B., ... Eissa, I. H. (2022). Modified benzoxazole-based VEGFR-2 inhibitors and apoptosis inducers: Design, synthesis, and anti-proliferative evaluation. *Molecules, 27*(15), 5047.

Erkkilä, O., Hernesniemi, J., & Tynkkynen, J. (2023). The association between digoxin use and long-term mortality after acute coronary syndrome. *The American Journal of Cardiology, 204*, 377–382.

Farghaly, H. S. M., Ashry, I. E. M., & Hareedy, M. S. (2018). High doses of digoxin increase the myocardial nuclear factor-kB and CaV1.2 channels in healthy mice. A possible mechanism of digitalis toxicity. *Biomedicine & Pharmacotherapy, 105*, 533–539.

Feng, X., Shi, Y., Xie, L., Zhang, K., Wang, X., Liu, Q., & Wang, P. (2019). 2-Deoxy-*D*-glucose augments photodynamic therapy induced mitochondrial caspase-independent apoptosis and energy-mediated autophagy. *Lasers in Surgery and Medicine, 51*(4), 352–362.

Fok, H., Victor, P., Bradberry, S., & Eddleston, M. (2018). Novel methods of self-poisoning: Repeated cardenolide poisoning after accessing *Cerbera odollam* seeds *via* the internet. *Clinical Toxicology, 56*(4), 304–306.

Fujii, T., Shimizu, T., Yamamoto, S., Funayama, K., Fujita, K., Tabuchi, Y., ... Sakai, H. (2018). Crosstalk between Na^+, K^+-ATPase and a volume-regulated anion channel in membrane microdomains of human cancer cells. *Biochimica et Biophysica Acta (BBA) - Molecular Basis of Disease, 1864*(11), 3792–3804.

Gaillard, Y., Krishnamoorthy, A., & Bevalot, F. (2004). *Cerbera odollam*: A 'suicide tree' and cause of death in the state of *Kerala*, India. *Journal of Ethnopharmacology, 95*(2–3), 123–126.

Geng, N., Jin, Y., Li, Y., Zhu, S., & Bai, H. (2020). AKR1B10 inhibitor epalrestat facilitates sorafenib-induced apoptosis and autophagy *via* targeting the mTOR pathway in hepatocellular carcinoma. *International Journal of Medical Sciences, 17*(9), 1246–1256.

Geng, X., Wang, F., Tian, D., Huang, L., Streator, E., Zhu, J., ... Tang, J. (2020). Cardiac glycosides inhibit cancer through Na/K-ATPase-dependent cell death induction. *Biochemical Pharmacology, 182*, 114226.

Ghanem, A., Ali, M. A., Elkady, M. A., Abdel Mageed, S. S., El Hassab, M. A., El-Ashrey, M. K., ... Doghish, A. S. (2023). *Rumex vesicarius* L. boosts the effectiveness of sorafenib in triple-negative breast cancer by downregulating BCl_2, mTOR, and JNK, and upregulating p21 expression. *Pathology - Research and Practice, 250*, 154807.

Gorantla, J. N., Vellekkatt, J., Nath, L. R., Anto, R. J., & Lankalapalli, R. S. (2014). Cytotoxicity studies of semi-synthetic derivatives of theveside derived from the aqueous extract of leaves of 'suicide tree' *Cerbera odollam*. *Natural Product Research, 28*(18), 1507–1512.

Hao, Y., Song, T., Wang, M., Li, T., Zhao, C., Li, T., ... He, H. (2023). Dual targets of lethal apoptosis and protective autophagy in liver cancer with periplocymarin elicit a limited therapeutic effect. *International Journal of Oncology, 62*(3), 44.

He, M., Liao, Q., Liu, D., Dai, X., Shan, M., Yang, M., ... Lian, J. (2023). Dihydroergotamine mesylate enhances the anti-tumor effect of sorafenib in liver cancer cells. *Biochemical Pharmacology, 211*, 115538.

Hossan, M. S., Chan, Z. Y., Collins, H. M., Shipton, F. N., Butler, M. S., Rahmatullah, M., ... Bradshaw, T. D. (2019). Cardiac glycoside cerberin exerts anticancer activity through PI3K/AKT/mTOR signal transduction inhibition. *Cancer Letters, 453*, 57–73.

Hou, Y., Shang, C., Meng, T., & Lou, W. (2021). Anticancer potential of cardiac glycosides and steroid-azole hybrids. *Steroids, 171*, 108852.

Hsu, C., Lin, L. I., Cheng, Y. C., Feng, Z. R., Shao, Y. Y., Cheng, A. L., & Ou, D. L. (2016). Cyclin E1 inhibition can overcome sorafenib resistance in hepatocellular carcinoma cells through Mcl-1 suppression. *Clinical Cancer Research, 22*(10), 2555–2564.

Hu, J. M., Chang, Y. L., Hsieh, C. C., & Huang, S. M. (2022). The synergistic cytotoxic effects of GW5074 and sorafenib by impacting mitochondrial functions in human colorectal cancer cell lines. *Frontiers in Oncology, 12*, 925653.

Hu, Z., Zhao, Y., Li, L., Jiang, J., Li, W., Mang, Y., ... Zhang, S. (2023). Metformin promotes ferroptosis and sensitivity to sorafenib in hepatocellular carcinoma cells *via* ATF4/STAT3. *Molecular Biology Reports, 50*(8), 6399–6413.

Hussain, Y., Meena, A., & Sinha, R. A. (2023). Gossypol synergises antiproliferative effect of sorafenib in metastatic lung cancer cells following Chou-Talalay algorithm. *Toxicology in Vitro, 93*, 105666.

Hussain, Y., Singh, J., Meena, A., Sinha, R. A., & Luqman, S. (2023). Escin enhanced the efficacy of sorafenib by autophagy-mediated apoptosis in lung cancer cells. *Phytotherapy Research, 37*(10), 4819–4837.

Hussain, Y., Singh, J., Meena, A., Sinha, R. A., & Luqman, S. (2024). Escin-sorafenib synergy up-regulates LC3-II and p62 to induce apoptosis in hepatocellular carcinoma cells. *Environmental Toxicology, 39*(2), 840–856.

Ismail, M. M. F., Shawer, T. Z., Ibrahim, R. S., Abusaif, M. S., Kamal, M. M., Allam, R. M., & Ammar, Y. A. (2023). Novel quinoxaline-3-propanamides as VGFR-2 inhibitors and apoptosis inducers. *RSC Advances, 13*(45), 31908–31924.

Jia, B., Zheng, X., Wu, M. L., Tian, X. T., Song, X., Liu, Y. N., ... Liu, J. (2021). Increased reactive oxygen species and distinct oxidative damage in resveratrol-suppressed glioblastoma cells. *Journal of Cancer, 12*(1), 141–149.

Jia, X. B., Zhang, Q., Xu, L., Yao, W. J., & Wei, L. (2021). Lotus leaf flavonoids induce apoptosis of human lung cancer A549 cells through the ROS/p38 MAPK pathway. *Biological Research, 54*(1), 7.

Kang, J. I., Hong, J. Y., Choi, J. S., & Lee, S. K. (2016). Columbianadin inhibits cell proliferation by inducing apoptosis and necroptosis in HCT116 colon cancer cells. *Biomolecules & Therapeutics, 24*(3), 320–327.

Kang, K. A., Yao, C. W., Piao, M. J., Zhen, A. X., Fernando, P. D. S. M., Herath, H. M. U. L., ... Hyun, J. W. (2022). Anticolon cancer effect of Korean red ginseng *via* autophagy- and apoptosis-mediated cell death. *Nutrients, 14*(17), 3558.

Kassop, D., Donovan, M. S., Cohee, B. M., Mabe, D. L., Wedam, E. F., & Atwood, J. E. (2014). An unusual case of cardiac glycoside toxicity. *International Journal of Cardiology, 170*(3), 434–437.

Kim, L. H., Shin, J. A., Jang, B., Yang, I. H., Won, D. H., Jeong, J. H., ... Cho, S. D. (2017). Sorafenib potentiates ABT-737-induced apoptosis in human oral cancer cells. *Archives of Oral Biology, 73*, 1–6.

Kim, M. J., Hwang, G. Y., Cho, M. J., Chi, B. H., Park, S. I., Chang, I. H., & Whang, Y. M. (2019). Depletion of NBR1 in urothelial carcinoma cells enhances rapamycin-induced apoptosis through impaired autophagy and mitochondrial dysfunction. *Journal of Cellular Biochemistry, 120*(11), 19186–19201.

Kuo, J. Y., Liao, C. L., Ma, Y. S., Kuo, C. L., Chen, J. C., Huang, Y. P., ... Chung, J. G. (2022). Combination treatment of sorafenib and bufalin induces apoptosis in NCI-H292 human lung cancer cells *in vitro*. *In Vivo, 36*(2), 582–595.

Laphookhieo, S., Cheenpracha, S., Karalai, C., Chantrapromma, S., Rat-a-pa, Y., Ponglimanont, C., & Chantrapromma, K. (2004). Cytotoxic cardenolide glycoside from the seeds of *Cerbera odollam*. *Phytochemistry, 65*(4), 507–510.

Li, H., Yu, Y., Liu, Y., Luo, Z., Law, B. Y. K., Zheng, Y., ... Li, W. (2022). Ursolic acid enhances the antitumor effects of sorafenib associated with Mcl-1-related apoptosis and SLC7A11-dependent ferroptosis in human cancer. *Pharmacological Research, 182*, 106306.

Li, R. S., Li, L. Y., Zhu, X. F., Li, X., Wang, C. Y., Qiu, S. J., ... Mu, Q. (2024). Annonaceous acetogenins synergistically inhibit hepatocellular carcinoma with sorafenib. *Journal of Natural Products, 87*(1), 14–27.

Li, X., Zheng, J., Chen, S., Meng, F. D., Ning, J., & Sun, S. L. (2021a). Oleandrin, a cardiac glycoside, induces immunogenic cell death *via* the PERK/elF2α/ATF4/CHOP pathway in breast cancer. *Cell Death & Disease, 12*(4), 314.

Li, Y., Xia, J., Shao, F., Zhou, Y., Yu, J., Wu, H., ... Ren, X. (2021b). Sorafenib induces mitochondrial dysfunction and exhibits synergistic effect with cysteine depletion by promoting HCC cells ferroptosis. *Biochemical and Biophysical Research Communications, 534*, 877–884.

Li, Z. J., Dai, H. Q., Huang, X. W., Feng, J., Deng, J. H., Wang, Z. X., ... Lu, G. D. (2021c). Artesunate synergizes with sorafenib to induce ferroptosis in hepatocellular carcinoma. *Acta Pharmacologica Sinica, 42*(2), 301–310.

Lim, J. G., Park, H. M., & Yoon, K. S. (2020). Analysis of saponin composition and comparison of the antioxidant activity of various parts of the quinoa plant (*Chenopodium quinoa* Willd.). *Food Science & Nutrition, 8*(1), 694–702.

Liu, J., Li, S. M., Tang, Y. J., Cao, J. L., Hou, W. S., Wang, A. Q., ... Jin, C. H. (2024). Jaceosidin induces apoptosis and inhibits migration in AGS gastric cancer cells by regulating ROS-mediated signaling pathways. *Redox Report, 29*(1), 2313366.

Liu, M., Huang, Q., Jun, A., Li, L., Li, X., Zhang, Z., & Dong, J. T. (2021). The cardiac glycoside deslanoside exerts anticancer activity in prostate cancer cells by modulating multiple signaling pathways. *Cancers, 13*(22), 5809.

Liu, S. H., Yu, J., Creeden, J. F., Sutton, J. M., Markowiak, S., Sanchez, R., ... Brunicardi, F. C. (2020). Repurposing metformin, simvastatin and digoxin as a combination for targeted therapy for pancreatic ductal adenocarcinoma. *Cancer Letters, 491*, 97–107.

Liu, Z., Wang, N., Meng, Z., Lu, S., & Peng, G. (2023). Pseudolaric acid B triggers cell apoptosis by activating AMPK/JNK/DRP1/mitochondrial fission pathway in hepatocellular carcinoma. *Toxicology, 493*, 153556.

Lu, G. Y., Liu, S. T., Huang, S. M., Chang, Y. L., & Lin, W. S. (2014). Multiple effects of digoxin on subsets of cancer-associated genes through the alternative splicing pathway. *Biochimie, 106*, 131–139.

Ma, Z., Chen, W., Liu, Y., Yu, L., Mao, X., Guo, X., ... Zhang, Y. (2024). Artesunate Sensitizes human hepatocellular carcinoma to sorafenib *via* exacerbating AFAP1L2-SRC-FUNDC1 axis-dependent mitophagy. *Autophagy, 20*(3), 541–556.

Maharana, P. K. (2021). Ethnobotanical, phytochemical, and pharmacological properties of *Cerbera manghas* L. *Journal of Biosciences, 46*(1), 25.

Martínez-Torres, A. C., Reyes-Ruiz, A., Calvillo-Rodriguez, K. M., Alvarez-Valadez, K. M., Uscanga-Palomeque, A. C., Tamez-Guerra, R. S., & Rodríguez-Padilla, C. (2020). IMMUNEPOTENT CRP induces DAMPS release and ROS-dependent autophagosome formation in HeLa and MCF-7 cells. *BMC Cancer, 20*(1), 647.

McConkey, D. J., Lin, Y., Nutt, L. K., Ozel, H. Z., & Newman, R. A. (2000). Cardiac glycosides stimulate Ca^{2+} increases and apoptosis in androgen-independent, metastatic human prostate adenocarcinoma cells. *Cancer Research, 60*(14), 3807–3812.

Medina-Meza, I. G., Aluwi, N. A., Saunders, S. R., & Ganjyal, G. M. (2016). GC-MS profiling of triterpenoid saponins from 28 quinoa varieties (*Chenopodium quinoa* Willd.) grown in Washington State. *Journal of Agricultural and Food Chemistry, 64*(45), 8583–8591.

Menezes, R. G., Usman, M. S., Hussain, S. A., Madadin, M., Siddiqi, T. J., Fatima, H., ... Luis, S. A. (2018). *Cerbera odollam* toxicity: A review. *Journal of Forensic and Legal Medicine, 58*, 113–116.

Menon, M. S., Kumar, P., & Jayachandran, C. I. (2016). Clinical profile and management of poisoning with suicide tree: An observational study. *Heart Views, 17*(4), 136–139.

Misek, R., Allen, G., LeComte, V., & Mazur, N. (2018). Fatality following intentional ingestion of *Cerbera odollam* seeds. *Clinical Practice and Cases in Emergency Medicine, 2*(3), 223–226.

Mondal, A., & Bennett, L. L. (2016). Resveratrol enhances the efficacy of sorafenib mediated apoptosis in human breast cancer MCF7 cells through ROS, cell cycle inhibition, caspase 3 and PARP cleavage. *Biomedicine & Pharmacotherapy, 84*, 1906–1914.

Muk, B., Vámos, M., Bógyi, P., Szabó, B., Dékány, M., Vágány, D., ... Nyolczas, N. (2020). The impact of serum concentration-guided digoxin therapy on mortality of heart failure patients: A long-term follow-up, propensity-matched cohort study. *Clinical Cardiology, 43*(12), 1641–1648.

Nagao, Y., Yokoi, A., Yoshida, K., Sugiyama, M., Watanabe, E., Nakamura, K., ... Kajiyama, H. (2023). Novel therapeutic strategies targeting UCP2 in uterine leiomyosarcoma. *Pharmacological Research, 189*, 106693.

Nordt, S. P., Hendrickson, M., Won, K., Miller, M. J., Swadron, S. P., & Cantrell, F. L. (2020). Death from cardiac glycoside "pong-pong" following use as weight-loss supplement purchased on Internet. *The American Journal of Emergency Medicine, 38*(8), 1698.e5–1698.e6.

Omar, H. A., Tolba, M. F., Hung, J. H., & Al-Tel, T. H. (2016). OSU-2S/sorafenib synergistic antitumor combination against hepatocellular carcinoma: The role of PKCδ/p53. *Frontiers in Pharmacology, 7*, 463.

Qin, S., Bi, F., Gu, S., Bai, Y., Chen, Z., Wang, Z., ... Chen, F. (2021). Donafenib versus sorafenib in first-line treatment of unresectable or metastatic hepatocellular carcinoma: A randomized, open-label, parallel-controlled phase II-III trial. *Journal of Clinical Oncology, 39*(27), 3002–3011.

Renymol, B., Palappallil, D. S., & Ambili, N. R. (2018). Study on clinical profile and predictors of mortality in *Cerbera odollam* poisoning. *Indian Journal of Critical Care Medicine, 22*(6), 431–434.

Reyes, R., Wani, N. A., Ghoshal, K., Jacob, S. T., & Motiwala, T. (2017). Sorafenib and 2-deoxyglucose synergistically inhibit proliferation of both sorafenib-sensitive and-resistant HCC cells by inhibiting ATP production. *Gene Expression, 17*(2), 129–140.

Riganti, C., Campia, I., Polimeni, M., Pescarmona, G., Ghigo, D., & Bosia, A. (2009). Digoxin and ouabain induce *P*-glycoprotein by activating calmodulin kinase II and hypoxia-inducible factor-1α in human colon cancer cells. *Toxicology and Applied Pharmacology, 240*(3), 385–392.

Rong, L., Li, Z., Leng, X., Li, H., Ma, Y., Chen, Y., & Song, F. (2020). Salidroside induces apoptosis and protective autophagy in human gastric cancer AGS cells through the PI3K/Akt/mTOR pathway. *Biomedicine & Pharmacotherapy, 122*, 109726.

Roskoski, R. Jr, (2024). Combination immune checkpoint and targeted protein kinase inhibitors for the treatment of renal cell carcinomas. *Pharmacological Research, 203*, 107181.

Rotella, J. A., Wong, O., Wong, A. Y., & Graudins, A. (2020). Overdose of pong pong (*Cerbera odollam*) seeds bought over the internet. *Emergency Medicine Australasia, 32*(2), 358–360.

Ru, R., Chen, G., Liang, X., Cao, X., Yuan, L., & Meng, M. (2023). Sea cucumber derived triterpenoid glycoside frondoside A: A potential anti-bladder cancer drug. *Nutrients, 15*(2), 378.

Sawong, S., Pekthong, D., Suknoppakit, P., Winitchaikul, T., Kaewkong, W., Somran, J., ... Srisawang, P. (2022). *Calotropis gigantea* stem bark extracts inhibit liver cancer induced by diethylnitrosamine. *Scientific Reports, 12*(1), 12151.

Saxena, M., Jadhav, E. B., Sankhla, M. S., Singhal, M., Parihar, K., Awasthi, K. K., & Awasthi, G. (2023). Bintaro (*Cerbera odollam* and *Cerbera manghas*): An overview of its eco-friendly use, pharmacology, and toxicology. *Environmental Science and Pollution Research, 30*(28), 71970–71983.

She, X., Yin, D., Guo, Q., Tang, Y., Wang, S., & Wang, X. (2024). Electrolyte disorders induced by six multikinase inhibitors therapy for renal cell carcinoma: A large-scale pharmacovigilance analysis. *Scientific Reports, 14*(1), 5592.

Shen, S., Zhang, Y., Wang, Z., Zhang, R., & Gong, X. (2014). Bufalin induces the interplay between apoptosis and autophagy in glioma cells through endoplasmic reticulum stress. *International Journal of Biological Sciences, 10*(2), 212–224.

Sikdar, S., Mukherjee, A., Ghosh, S., & Khuda-Bukhsh, A. R. (2014). Condurango glycoside-rich components stimulate DNA damage-induced cell cycle arrest and ROS-mediated caspase-3 dependent apoptosis through inhibition of cell-proliferation in lung cancer, *in vitro* and *in vivo*. *Environmental Toxicology and Pharmacology, 37*(1), 300–314.

Silva, L. N. D., Pessoa, M. T. C., Alves, S. L. G., Venugopal, J., Cortes, V. F., Santos, H. L., ... Barbosa, L. A. (2017). Differences of lipid membrane modulation and oxidative stress by digoxin and 21-benzylidene digoxin. *Experimental Cell Research, 359*(1), 291–298.

Şirin, N., Elmas, L., Seçme, M., & Dodurga, Y. (2020). Investigation of possible effects of apigenin, sorafenib and combined applications on apoptosis and cell cycle in hepatocellular cancer cells. *Gene, 737*, 144428.

Song, J., Ham, J., Park, W., Song, G., & Lim, W. (2024). Osthole impairs mitochondrial metabolism and the autophagic flux in colorectal cancer. *Phytomedicine, 125*, 155383.

Sun, L., Jiang, Y., Yan, X., Dai, X., Huang, C., Chen, L., ... Lian, J. (2021). Dichloroacetate enhances the anti-tumor effect of sorafenib *via* modulating the ROS-JNK-Mcl-1 pathway in liver cancer cells. *Experimental Cell Research, 406*(1), 112755.

Sun, Y., Zhang, H., Meng, J., Guo, F., Ren, D., Wu, H., & Jin, X. (2022). *S*-Palmitoylation of PCSK9 induces sorafenib resistance in liver cancer by activating the PI3K/AKT pathway. *Cell Reports, 40*(7), 111194.

Taha, A. M., Aboulwafa, M. M., Zedan, H., & Helmy, O. M. (2022). Ramucirumab combination with sorafenib enhances the inhibitory effect of sorafenib on HepG2 cancer cells. *Scientific Reports, 12*(1), 17889.

Talezadeh Shirazi, P., Farjadian, S., Dabbaghmanesh, M. H., Jonaidi, H., Alavianmehr, A., Kalani, M., & Emadi, L. (2022). Eugenol: A new option in combination therapy with sorafenib for the treatment of undifferentiated thyroid cancer. *Iranian Journal of Allergy, Asthma, and Immunology, 21*(3), 313–321.

Tang, W., Chen, Z., Zhang, W., Cheng, Y., Zhang, B., Wu, F., ... Wang, X. (2020). The mechanisms of sorafenib resistance in hepatocellular carcinoma: Theoretical basis and therapeutic aspects. *Signal Transduction and Targeted Therapy, 5*(1), 87.

Trenti, A., Grumati, P., Cusinato, F., Orso, G., Bonaldo, P., & Trevisi, L. (2014). Cardiac glycoside ouabain induces autophagic cell death in non-small cell lung cancer cells *via* a JNK-dependent decrease of Bcl-2. *Biochemical Pharmacology, 89*(2), 197–209.

Üremiş, M. M., Üremiş, N., & Türköz, Y. (2023). Cucurbitacin E shows synergistic effect with sorafenib by inducing apoptosis in hepatocellular carcinoma cells and regulates Jak/Stat3, ERK/MAPK, PI3K/Akt/mTOR signaling pathways. *Steroids, 198*, 109261.

Vishnoi, K., Ke, R., Viswakarma, N., Srivastava, P., Kumar, S., Das, S., ... Rana, B. (2022). Ets1 mediates sorafenib resistance by regulating mitochondrial ROS pathway in hepatocellular carcinoma. *Cell Death & Disease, 13*(7), 581.

Walker, T., Mitchell, C., Park, M. A., Yacoub, A., Graf, M., Rahmani, M., ... Dent, P. (2009). Sorafenib and vorinostat kill colon cancer cells by CD95-dependent and-independent mechanisms. *Molecular Pharmacology, 76*(2), 342–355.

Wang, G. Y., Zhang, L., Geng, Y. D., Wang, B., Feng, X. J., Chen, Z. L., ... Jiang, L. (2022a). β-Elemene induces apoptosis and autophagy in colorectal cancer cells through regulating the ROS/AMPK/mTOR pathway. *Chinese Journal of Natural Medicines, 20*(1), 9–21.

Wang, L., Wang, C., Tao, Z., Zhao, L., Zhu, Z., Wu, W., ... Chen, T. (2019). Curcumin derivative WZ35 inhibits tumor cell growth *via* ROS-YAP-JNK signaling pathway in breast cancer. *Journal of Experimental & Clinical Cancer Research, 38*(1), 460.

Wang, S. Y., Wei, Y. H., Shieh, D. B., Lin, L. L., Cheng, S. P., Wang, P. W., & Chuang, J. H. (2015). 2-Deoxy-*D*-glucose can complement doxorubicin and sorafenib to suppress the growth of papillary thyroid carcinoma cells. *PLoS One, 10*(7), e0130959.

Wang, T. T., Hong, Y. F., Chen, Z. H., Wu, D. H., Li, Y., Wu, X. Y., ... Jia, C. C. (2021). Synergistic effects of α-mangostin and sorafenib in hepatocellular carcinoma: New insights into α-mangostin cytotoxicity. *Biochemical and Biophysical Research Communications, 558*, 14–21.

Wang, X., Gupta, P., Jramne, Y., Danilenko, M., Liu, D., & Studzinski, G. P. (2020). Carnosic acid increases sorafenib-induced inhibition of ERK1/2 and STAT3 signaling which contributes to reduced cell proliferation and survival of hepatocellular carcinoma cells. *Oncotarget, 11*(33), 3129–3143.

Wang, X., Hu, R., Song, Z., Zhao, H., Pan, Z., Feng, Y., ... Zhang, J. (2022b). Sorafenib combined with STAT3 knockdown triggers ER stress-induced HCC apoptosis and cGAS-STING-mediated anti-tumor immunity. *Cancer Letters, 547*, 215880.

Wei, L., Lee, D., Law, C. T., Zhang, M. S., Shen, J., Chin, D. W., ... Wong, C. M. (2019). Genome-wide CRISPR/Cas9 library screening identified PHGDH as a critical driver for sorafenib resistance in HCC. *Nature Communications, 10*(1), 4681.

Wei, Q., Ren, Y., Zheng, X., Yang, S., Lu, T., Ji, H., ... Shan, K. (2022). Ginsenoside Rg3 and sorafenib combination therapy relieves the hepatocellular carcinomaprogression through regulating the HK2-mediated glycolysis and PI3K/Akt signaling pathway. *Bioengineered, 13*(5), 13919–13928.

Wen, S., Chen, Y., Lu, Y., Wang, Y., Ding, L., & Jiang, M. (2016). Cardenolides from the Apocynaceae family and their anticancer activity. *Fitoterapia, 112*, 74–84.

Wermuth, M. E., Vohra, R., Bowman, N., Furbee, R. B., & Rusyniak, D. E. (2018). Cardiac toxicity from intentional ingestion of pong-pong seeds (*Cerbera odollam*). *The Journal of Emergency Medicine, 55*(4), 507–511.

Wiczk, A., Hofman, D., Konopa, G., & Herman-Antosiewicz, A. (2012). Sulforaphane, a cruciferous vegetable-derived isothiocyanate, inhibits protein synthesis in human prostate cancer cells. *Biochimica et Biophysica Acta (BBA) - Molecular Cell Research, 1823*(8), 1295–1305.

Wilhelm, S., Carter, C., Lynch, M., Lowinger, T., Dumas, J., Smith, R. A., ... Kelley, S. (2006). Discovery and development of sorafenib: A multikinase inhibitor for treating cancer. *Nature Reviews Drug Discovery, 5*(10), 835–844.

Winitchaikul, T., Sawong, S., Surangkul, D., Srikummool, M., Somran, J., Pekthong, D., ... Srisawang, P. (2021). *Calotropis gigantea* stem bark extract induced apoptosis related to ROS and ATP production in colon cancer cells. *PLoS One, 16*(8), e0254392.

Wu, Q., Wang, X., Pham, K., Luna, A., Studzinski, G. P., & Liu, C. (2020). Enhancement of sorafenib-mediated death of Hepatocellular carcinoma cells by carnosic acid and vitamin D2 analog combination. *The Journal of Steroid Biochemistry and Molecular Biology, 197*, 105524.

Xiao, Y., Yan, W., Guo, L., Meng, C., Li, B., Neves, H., ... Lin, Y. (2017). Digitoxin synergizes with sorafenib to inhibit hepatocelluar carcinoma cell growth without inhibiting cell migration. *Molecular Medicine Reports, 15*(2), 941–947.

Xu, J., Ji, L., Ruan, Y., Wan, Z., Lin, Z., Xia, S., ... Cai, X. (2021). UBQLN1 mediates sorafenib resistance through regulating mitochondrial biogenesis and ROS homeostasis by targeting PGC1β in hepatocellular carcinoma. *Signal Transduction and Targeted Therapy, 6*(1), 190.

Yang, N. N., Zhang, J., Zhao, Y. L., Wang, Y. Z., & Zhao, Y. H. (2016). Distinguish and quality estimation of the leaves of *Alstonia scholaris* (L.) R. Br. from different harvest time based on the UV-Vis·FP and HPLC·FP. *Spectroscopy and Spectral Analysis, 36*(12), 4021–4027.

Yang, S., Yang, S., Zhang, H., Hua, H., Kong, Q., Wang, J., & Jiang, Y. (2021). Targeting Na^+/K^+-ATPase by berbamine and ouabain synergizes with sorafenib to inhibit hepatocellular carcinoma. *British Journal of Pharmacology, 178*(21), 4389–4407.

Yao, J., He, Z., Chen, J., Sun, W., Fang, H., & Xu, W. (2012). Design, synthesis and biological activities of sorafenib derivatives as antitumor agents. *Bioorganic & Medicinal Chemistry Letters, 22*(21), 6549–6553.

Yao, X., Zhao, C. R., Yin, H., Wang, K., & Gao, J. J. (2020). Synergistic antitumor activity of sorafenib and artesunate in hepatocellular carcinoma cells. *Acta Pharmacologica Sinica, 41*(12), 1609–1620.

Yuan, R., Zhao, W., Wang, Q. Q., He, J., Han, S., Gao, H., ... Yang, S. (2021). Cucurbitacin B inhibits non-small cell lung cancer *in vivo* and *in vitro* by triggering TLR4/NLRP3/GSDMD-dependent pyroptosis. *Pharmacological Research, 170*, 105748.

Yunos, N. M., Osman, A., Jauri, M. H., Sallehudin, N. J., & Mutalip, S. S. M. (2020). The *in vitro* anti-cancer activities of 17βh-neriifolin isolated from *Cerbera odollam*

and its binding activity on Na^+, K^+-ATPase. *Current Pharmaceutical Biotechnology, 21*(1), 37–44.
Zhang, R., Chen, Z., Wu, S. S., Xu, J., Kong, L. C., & Wei, P. (2019). Celastrol enhances the anti-liver cancer activity of sorafenib. *Medical Science Monitor, 25*, 4068–4075.
Zhang, R. Y., Zhang, X., Zhang, L., Wu, Y. C., Sun, X. J., & Li, L. (2021a). Tetrahydroxystilbene glucoside protects against sodium azide-induced mitochondrial dysfunction in human neuroblastoma cells. *Chinese Herbal Medicines, 13*(2), 255–260.
Zhang, Y., Ishida, C. T., Ishida, W., Lo, S. L., Zhao, J., Shu, C., ... Siegelin, M. D. (2018). Combined HDAC and bromodomain protein inhibition reprograms tumor cell metabolism and elicits synthetic lethality in glioblastoma. *Clinical Cancer Research, 24*(16), 3941–3954.
Zhang, Z., Wang, Y., Ma, Q., Zhang, S., Liu, H., Zhao, B., ... Kong, D. (2021b). Biomimetic carrier-free nanoparticle delivers digoxin and doxorubicin to exhibit synergetic antitumor activity *in vitro* and *in vivo*. *Chemical Engineering Journal, 406*, 126801.
Zheng, L., Fang, S., Chen, A., Chen, W., Qiao, E., Chen, M., ... Ji, J. (2022). Piperlongumine synergistically enhances the antitumour activity of sorafenib by mediating ROS-AMPK activation and targeting CPSF7 in liver cancer. *Pharmacological Research, 177*, 106140.
Zhou, C., Yu, T., Zhu, R., Lu, J., Ouyang, X., Zhang, Z., ... Hu, D. (2023). Timosaponin AIII promotes non-small-cell lung cancer ferroptosis through targeting and facilitating HSP90 mediated GPX4 ubiquitination and degradation. *International Journal of Biological Sciences, 19*(5), 1471–1489.
Zhou, J., Jiang, Y., Chen, H., Wu, Y., & Zhang, L. (2020). Tanshinone I attenuates the malignant biological properties of ovarian cancer by inducing apoptosis and autophagy via the inactivation of PI3K/AKT/mTOR pathway. *Cell Proliferation, 53*(2), e12739.
Zhou, Y., Zhou, Y., Yang, M., Wang, K., Liu, Y., Zhang, M., ... Hu, R. (2019). Digoxin sensitizes gemcitabine-resistant pancreatic cancer cells to gemcitabine *via* inhibiting Nrf2 signaling pathway. *Redox Biology, 22*, 101131.
Zhu, L., Wang, Y., Lv, W., Wu, X., Sheng, H., He, C., & Hu, J. (2021). Schizandrin A can inhibit non-small cell lung cancer cell proliferation by inducing cell cycle arrest, apoptosis and autophagy. *International Journal of Molecular Medicine, 48*(6), 214.
Zhu, X., Zhang, Y., Wang, Y., Zhang, H., Wang, X., Tang, H., ... Sun, L. (2022). Agrimoniin sensitizes pancreatic cancer to apoptosis through ROS-mediated energy metabolism dysfunction. *Phytomedicine, 96*, 153807.